ELSEVIER

Contents lists available at ScienceDirect

International Journal of Biological Macromolecules

journal homepage: www.elsevier.com/locate/ijbiomac





Use of emulsifying plant protein hydrolysates from winery, whiskey and brewery by-products for the development of echium oil delivery emulsions[★]

Mariana Sisconeto Bisinotto ^{a,b}, Inar Castro ^b, Julia Maldonado-Valderrama ^c, Nykola C. Jones ^d, Teresa del Castillo-Santaella ^e, Søren Vrønning Hoffmann ^d, Emilia M. Guadix ^a, Pedro J. García-Moreno ^{a,*}

- ^a Department of Chemical Engineering, University of Granada, Granada, Spain
- b LADAF, Pharmaceutical Science Faculty, University of Sao Paulo, Brazil
- ^c Department of Applied Physics, University of Granada, Granada, Spain
- d ISA, Department of Physics and Astronomy, Aarhus University, Aarhus, Denmark
- e Department of Physical Chemistry, University of Granada, Granada, Spain

ARTICLE INFO

Keywords: Emulsifying plant peptides Interfacial adsorption and rheology Barley spent grains Grape seed flour Synchrotron radiation circular dichroism Omega-3 fatty acids Lipid oxidation

ABSTRACT

This study investigates the production of plant protein hydrolysates from defatted grape seed flour and barley spent grains, by-products of wine, beer and whiskey industries, using limited hydrolysis with subtilisin or trypsin. The hydrolysates were characterized by protein content, molecular weight, antioxidant capacity, interfacial adsorption, dilatational rheology, and interfacial conformational changes using synchrotron radiation circular dichroism. Physical and oxidative stability of 5 % echium oil-in-water emulsions (pH 7), stabilized by the hydrolysates, were studied during seven days of storage. The trypsin-derived hydrolysate from brewers' spent grains resulted in the most physically stable emulsion due to enhanced interfacial adsorption and higher dilatational modulus. Alternatively, the trypsin-treated grape seed flour hydrolysate provided the emulsion with the highest oxidative stability, aligning with its superior *in vitro* antioxidant capacity. These results show the potential of wine and brewery industry side streams as a sustainable source of plant-based emulsifiers with application in omega-3 delivery systems.

1. Introduction

Cardiovascular diseases (CVD) are the leading cause of death worldwide, causing 18.6 million deaths in 2019 [1,2]. The underlying cause of CVD is atherosclerosis, and the consumption of omega-3 polyunsaturated fatty acids (n-3PUFA), mainly eicosapentaenoic (EPA, C20:5 n-3) and docosahexaenoic acid (DHA, C22:6 n-3), is related to a reduction in the residual risk of CVD [3,4]. The primary dietary sources of EPA and DHA are fish (e.g. sardine, mackerel, and anchovy) and fish oil supplements [5]. However, Western countries have a low fish intake, thus the development of appropriate omega-3 enriched food is necessary to meet nutritional requirements [6,7]. In addition, the global supply of seafood from wild capture fisheries is unlikely to meet the global needs of EPA and DHA of the world's increasing population [5]. Given this

unbalance between supply and demand, it is imperative to identify new sources of n-3PUFA and develop strategies to increase their consumption.

Plant based sources of alpha-linolenic (ALA, C18:3 n-3), such as flaxseed, chia, soybean, hemp, canola, have emerged as economical, dietary acceptable and sustainable alternative to fish oil and fish oil supplements [8]. This is because mammals can biosynthesize EPA and DHA from both ALA and stearidonic (SDA, C18:4 n-3) acids, with SDA being the more efficient precursor [9]. Therefore, non-conventional vegetable oils, like echium oil, have drawn attention due to the SDA content. Extracted from *Echium plantagineum* L. seeds, echium oil has a high content of n3PUFA, particularly 28 % of ALA and 12 % of SDA [10].

The biggest challenge to produce omega-3 enriched food for boosting n-3PUFA consumption, is to avoid lipid oxidation, which reduces oil's

^{*} This article is part of a special issue entitled: 'Protein-based delivery systems' published in International Journal of Biological Macromolecules.

^{*} Corresponding author at: Department of Chemical Engineering, Avenida de la Fuente Nueva S/N, Granada, Granada 18071, Spain. E-mail address: pjgarcia@ugr.es (P.J. García-Moreno).

nutritional value and product sensorial properties [11]. In this regard, oil-in-water (O/W) emulsions are commonly used as delivery systems for the incorporation of n3-PUFA into water-based food matrices [12]. In emulsions, the oil-water interface plays a central role in lipid oxidation since it is the place where pro-oxidant species (oxygen, free radicals and metal ions) encounter oil to start the oxidation process [13]. This is affected by many factors, such as droplet size, interface composition, presence of pro- and antioxidant compounds and emulsifier properties (interfacial viscoelasticity, net charge) [13–15].

Animal proteins are often used as natural emulsifiers in O/W emulsions due to their excellent amphiphilic properties. However, a huge research effort is being made to replace them with sustainable plant protein-based alternatives [16]. Moreover, this transition is not straightforward since most plant protein ingredients drastically differ from the commonly used animal proteins, such as dairy-derived ones, due to their insolubility in aqueous media [13]. Enzymatic hydrolysis is a safe, simple, and cheap method to improve the emulsifying and anti-oxidant capacity of plant proteins by increasing the plant protein solubility and interfacial activity by exposing buried hydrophobic groups [17,18]. Side-stream products from food industry (e.g., wineries and breweries) are sustainable, low-cost and available sources of plant proteins, and therefore adding value to these by-products is of utmost relevance [18–20].

First, wineries produce 10 million tons per year of grape pomace, which is used as raw material for fertilizers, animal feed [22] and wine alcohol production. Moreover, the production of grape seed oil, generates defatted grape seed flour with a content of 10-11 % protein [21]. There are previous studies optimizing the extraction of grape seed protein, which have reported some emulsifying activity for the protein extracts [21,25]. Nevertheless, and to our knowledge, there are no works in the literature evaluating the use of enzymatic hydrolysis to produce grape seed protein hydrolysates with combined emulsifying and antioxidant capacity. Secondly, brewers dispose 40 million tons of wet brewer's spent grain annually in the world, being traditionally used as animal feed due to its high protein content (around 20 %) [20,23]. Extensive efforts have been made to increase the value of spent grains by using them as a food ingredient to fortify pasta and bakery products due to their high protein and fibre content [24]. Although other authors have reported the emulsifying activity of protein hydrolysates obtained from spent grains [26-28], the interfacial properties of the hydrolysates, as well as the physical and oxidative stability of the resulting emulsions, have not yet been studied.

In light of the above, the aims of this study were (i) to produce and characterize plant-protein hydrolysates obtained by limited enzymatic hydrolysis of defatted grape seed flour and barley spent grains from whiskey and beer production (ii) to evaluate the interfacial properties (interfacial adsorption, dilatational rheology and interfacial conformational changes) as well as the in vitro antioxidant capacity of the obtained hydrolysates (iii) to investigate the physical and oxidative stability of 5 % echium oil-in-water emulsions stabilized with the obtained hydrolysates. Thus, this work provides new insights into the interfacial properties of plant protein hydrolysates and their emulsifying and antioxidant capacity, which are of special relevance for the physical and chemical stabilization of omega-3 delivery emulsions.

2. Materials and methods

2.1. Materials

Defatted grape seed flour was kindly donated by Agralco S. Coop. (Navarra, Spain). A 100 % malted barley spent grain from whiskey production was kindly donated by Liber Distillery (Granada, Spain). A non-malted barley spent grain from beer production was kindly donated by Alhambra Brewery (Granada, Spain). Alcalase 2.4 L (subtilisin EC 3.4.21.62) and PTN 6.0S (trypsin 3.4.21.4) were supplied by Novozymes (Bagsvaerd, Denmark). Refined echium oil was purchased from De Wit

Speciality Oils (De Waal, Tescel, The Netherlands) and kept at $-80\,^{\circ}\text{C}$ until use. The supplier reports an addition of 1000 ppm of mixed tocopherols (\$\alpha\$-tocopherol: 7–14 %; \$\beta\$-tocopherol: 1–3 %; \$\gamma\$-tocopherol: 35–46 %; \$\delta\$-tocopherol: 14–20 %). Previous studies regarding the stability of this refined echium oil identified delta, gamma and alfatocopherols (439.78 \pm 0.42, 1016.44 \pm 0.43 and 139.09 \pm 0.43 mg/kg oil, respectively) [10]. In addition, endogenous gamma-tocopherol was identified in echium oil extracted directly from *Echium plantagineum* L. seeds (in a range of 536.9 \pm 0.22 to 782.24 \pm 6.35 mg/kg oil) [29,30]. Reagents (ferrozine, p-anisidine, ferrous chloride, 2-diphenyil-picrylhydrazyl (DPPH)) were purchased from Sigma-Aldrich.

2.2. Pretreatment and hydrolysis of side-stream products

2.2.1. Drying and inactivation of endogenous enzymes

Barley spent grains have a high moisture content (70–80 %), making it susceptible to spoilage and deterioration [31]. Hence, 100 % malted and non-malted barley spent grains from whiskey and beer production (W and B, respectively) were divided into three small portions (approx. 10 kg) and each portion was dried at 100 °C for 8 h to extend microbiology and chemical stability until hydrolysis analysis. Thus, the dried materials were milled using a Knifetec 1095 (Foss Tecator, Hoganas, SE) before hydrolysis. The defatted grape seed flour (G) was hydrolyzed as supplied. The three raw materials (G, W, B) were kept at 8 °C until hydrolysis and their moisture were determined by infrared moisture determination balance (AD-4714.2, A&D Company, Tokyo, JPN).

To evaluate the activity of endogenous enzymes, an aqueous solution at 2.5 % wt. protein concentration of all raw materials was placed into a stirred tank reactor under hydrolysis conditions (50 °C, pH 8.0) without any commercial enzyme addition [32]. An automatic titrator 718 Stat Titrino (Metrohm, Herisau, Switzerland) was used to keep the pH constant by addition of 1 M NaOH. If endogenous enzyme activity was confirmed, a thermal deactivation treatment (90 °C, 15 min) was performed before enzymatic hydrolysis.

2.2.2. Enzymatic hydrolysis

The hydrolysis was performed as described by García-Moreno et al. (2016) [33], with some modifications. An aqueous solution at 2.5 % wt. protein concentration was pre-heated in a hot water bath (90 $^{\circ}$ C, 15 min) before being placed into a stirred tank reactor to adjust the hydrolysis conditions (50 $^{\circ}$ C, pH 8.0). Subsequently, subtilisin or trypsin enzymes were added at the enzyme/subtract ratio (E/S) of 0.5 wt%, and the hydrolysis was conducted until the degree of hydrolysis (DH) of 5 % was obtained, which was calculated according to the pH-stat method [37] described by Eq. (1).

$$DH = \frac{Nb \times Vb}{Mp} \frac{1}{\alpha} \frac{1}{htot} 100 \text{ with } \alpha = \frac{\left(10^{pH-pK}\right)}{1 - 10^{pH-pK}}$$
 (1)

where: (DH) degree of hydrolysis; (Nb) base normality; (Vb) volume of base consumed; (Mp) protein mass in the reactor; (h_{tot}) total number of peptide bonds present (8.6); (α) Average degree of dissociation of α -amino groups at 50 °C; reaction pH 8.0 and average pK of the released α -amino groups (7.177).

Subtilisin, EC 3.4.21.62, of bacterial origin (Alcalase 2.4 L) and trypsin, EC 3.4.21.4, from animal sources (PTN 6.0S) were used in this work since they are widely employed commercial proteases, which have been previously reported in numerous studies to produce protein hydrolysates exhibiting emulsifying activity [15,34–36]. Hydrolysates production with a low degree of hydrolysis (DH = 5 %) was targeted to obtain peptides retaining a relatively large size and optimal balance between hydrophilic and hydrophobic amino acid residues, which facilitates their ability to adsorb and unfold at the oil/water interface [15].

After the hydrolysis, the reaction mixture was heated ($90 \,^{\circ}$ C, $15 \,^{\circ}$ min) to inactivate the added enzyme and cooled at room temperature in an iced water bath. The hydrolysate was centrifuged (Z 206 A, Hermle,

Germany) at 770 x g for 15 min, and the supernatant was filtered in an 8 mm paper filter under vacuum to be subsequently freeze-dried and stored at $-20\,^{\circ}\text{C}$ until further analysis. The obtained hydrolysates were coded as follows: defatted grape seed flour (G) hydrolyzed by subtilisin or trypsin (GS and GT), 100 % of malted barley spent grains from whiskey production (W) hydrolyzed by subtilisin or trypsin (WS and WT), and 100 % non-malted barley spent grains from beer production (B) hydrolyzed by subtilisin or trypsin (BS and BT).

2.2.3. Protein yield from enzymatic hydrolysis

The efficiency of each enzymatic treatment to release solids from the original matrix and solubilize plant protein was expressed as total solids recovery and plant protein solubility, as described by Eqs. (2) and (3):

Total solids recovery (%) =
$$\left(M_{h/M_{t}}\right) \times 100$$
 (2)

where M_h represents the total mass of freeze-dried hydrolysate obtained, while M_t is the total mass of side-stream product used to produce the hydrolysate.

Plant protein solubility (%) =
$$\left(\left(m_{hp} \times M_h\right)/\left(m_{tp} \times M_t\right)\right) \times 100$$
 (3)

where m_{hp} represents the protein content of the hydrolysate and M_h is the total mass of freeze-dried hydrolysate obtained, m_{tp} represents the total crude protein of the original side-stream product and M_t is the total mass of side-stream product used to produce the hydrolysate.

2.3. Characterization of raw materials and hydrolysates

2.3.1. Protein content

The protein content of all side stream products and respective hydrolysates were determined by the AOAC method (997.09) [38], assuming a nitrogen-to-protein conversion factor of 6.25. Measurements were performed in triplicate, and results expressed as mean \pm standard deviation.

2.3.2. Isoelectric point

The isoelectric point of the plant protein hydrolysates was determined by automatic titration with 0.5 M NaOH, 0.1 M and 1 M HCl in Zetasizer Nano ZS (Malvern Instruments Ltd., Worcestershire, UK). The assay was performed in triplicate and the results were expressed as mean \pm standard deviation.

2.3.3. Amino acid profile

The amino acid profiles were determined using an automatic amino acid analyzer Biochrom 30+ (Biochrom, Cambridge, UK) according to Lazarević et al. (2022) [39]. First, samples were diluted, norleucine was added as an internal standard, and acid hydrolysis was carried out with 6 M HCl (110 °C for 21 h). After cooling down at room temperature, the solution was dried at Speed Vac and resuspended in sodium citrate loading buffer (pH 2.2) (Biochrom, Cambridge, UK) at a final volume of $25\,\text{mL}$. Then, it was filtered with $0.22\,\mu\text{m}$ PTFE filter and transferred into a vial (Agilent Technologies, Santa Clara, CA, USA) to be injected into the strong ion exchange chromatography column to separate the amino acids. The eluent was mixed with ninhydrin, which, in the presence of the separated amino acids, resulted in coloured compounds being photometrically detected. All amino acids were detected at 570 nm, except for proline, which was detected at 440 nm. The identification was made by comparison of the sample peak retention time to the retention time of the Amino Acid Standard Solution kit (Sigma-Aldrich, St. Louis, MI, USA). The quantification was carried out based on calibration curves of standards for each amino acid in molar percentage. Measurements were carried out in triplicate, and the results were expressed as mean \pm standard deviation.

2.3.4. Molecular weight distribution of hydrolysates

Molecular weight distribution was performed according to Bisinotto et al. (2021) [40]. The hydrolysates (5 mg of protein/mL) were solubilized in a sodium phosphate buffer (25 mM pH 7.4 with 150 mM NaCl) and sonicated for 10 min. Then, the solution was filtered through a 0.45 and 0.22 µm Nylon filter before injection (500 µL) into the column Superdex 30 Increase 10/300 GL (GE Healthcare, Chicago, Illinois, USA). The same buffer was used as the mobile phase in an isocratic flow rate of 0.5 mL/min. The detection was performed at 280 nm in a Size-Exclusion Chromatography, SEC (AKTA Purifier, GE Healthcare, Chicago, Illinois, USA) equipped with Unicorn 5.11 Software. The molecular weight was determined by comparison to a calibration curve built up with the following standard compounds: L-Tyrosine (217.7 Da), Vitamin B12 (1355.37 Da), Insulin (5807.6 Da), Ribonuclease A (13,700 Da) (Sigma-Aldrich, St. Louis, MI, USA). Measurements were carried out in duplicate and expressed as the percentage of area under the curve.

2.4. Determination of in vitro antioxidant capacity

2.4.1. 2,2-Diphenyil-picrylhydrazyl (DPPH) radical scavenging capacity

The DPPH radical scavenging capacity of the hydrolysates was determined as the IC $_{50}$ value, which represents the hydrolysate concentration (mg protein/mL) that inhibits 50 % of DPPH activity [41]. For this purpose, an aqueous solution of each hydrolysate and its serial dilution (from 0.6 to 0.01 mg protein/mL) were prepared. Thus, 1 mL of the hydrolysate aqueous solution was mixed with 1 mL of 0.1 mM DPPH methanolic solution, stirred for 1 min and left to react for 30 min at room temperature in the dark. Afterwards, the absorbance was read in a spectrophotometer at 515 nm (Asample). Sample control for each hydrolysate aqueous solution concentration were run following the same protocol by adding 1 mL of methanol instead of the DPPH solution (Asample control), and a blank reaction was made by adding 1 mL of distilled water instead of hydrolysate solution (Ablank). A triplicate of measurement was performed, and the percentage of DPPH inhibition was calculated as follows:

DPPH inhibition (%) =
$$\left(1 - \left(\frac{\left(A_{sample} - A_{sample\ control}\right)}{A_{blank}}\right)\right) \times 100$$
 (4)

The natural logarithm of sample concentration was plotted against the percentage of DPPH inhibition. Thus, from the linear region of the curve, the half maximal inhibitory concentration (IC50) was calculated from the linear equation. The results were expressed as mean \pm standard deviation.

2.4.2. Iron (Fe⁺²) chelating capacity

The capacity of each hydrolysate to chelate ferrous ions (Fe^{2+}) was measured as previously described by García-Moreno et al. (2014) [41]. In short, two falcon tubes were prepared for each sample reaction, where 1 mL of sample (hydrolysate aqueous solution in different concentrations from 2 to 0.1 mg protein/mL) was added to 3.7 mL of distilled water and 0.1 mL of 2 mM ferrous chloride aqueous solution. The total volume was stirred vigorously for 10 s and left to react for 3 min at room temperature. Then, 0.2 mL of 5 mM ferrozine aqueous solution was added to one of the falcon tubes (sample tube), and 0.2 mL of distilled water was added to the second falcon tube (sample control tube). The mixture was stirred vigorously for 10 s and left to react for 10 min at room temperature before the absorbance was read at 562 nm. A blank was filled with distilled water instead of hydrolysate aqueous solution. The measurements were done in triplicate, and the iron chelating capacity was calculated as follows:

Iron chelating activity (%) =
$$\left(1 - \left(\frac{\left(A_{sample} - A_{sample \ control}\right)}{A_{blank}}\right) \times 100$$
 (5)

The natural logarithm of sample concentration was plotted against the percentage of iron chelating capacity. Therefore, from the linear region of the curve, the half maximal inhibitory concentration (IC $_{50}$) was calculated from the linear equation. The results were expressed as mean \pm standard deviation.

2.5. Determination of interfacial properties

2.5.1. Synchrotron radiation circular dichroism (SRCD)

SRCD measurements were carried out on the AU-CD beamline at the ASTRID2 synchrotron radiation source, (ISA, Department of Physics & Astronomy, Aarhus University in Denmark) to investigate the conformational changes in the secondary structure of peptides from the hydrolysates when they are (a) solubilized in buffer solution to (b) being adsorbed at the oil-water interface in O/W emulsions [14]. Measurements were carried out similarly to our previous works [15,42]. As usual, the calibration of the SRCD spectrometer was confirmed daily using camphorsulfonic acid for optical rotation magnitude and wavelength [43]. A 0.01 cm path length quartz Suprasil cell (Hellma GmbH & Co., Germany) was used for far-UV SRCD measurements at 25 °C. The far-UV SRCD spectra were recorded in triplicate from 280 to 170 nm in 1 nm steps, with a dwell time of 2 s per point.

First, a stock solution of each hydrolysate was prepared by diluting the hydrolysate in 10 mM phosphate buffer pH 7, stirring for at least 4 h, or overnight, when possible, at room temperature. Then, the stock solution was added to the buffer until 2%wt. of protein (protein solution). For SRCD measurements, the protein solutions were further diluted (1:22, v/v) in the same buffer to reduce absorbance.

Second, an oil-in-water (O/W) emulsions were produced by dispersing 5 wt% tricaprylin oil in the stock solution of each hydrolysate to the final concentration of 2 wt% of protein. A 30 s prehomogenization in Polytron™ PT 1200E at 18,000 rpm (Kinematica AG, Malters, CHE) was performed, followed by a secondary homogenization using a Q125 sonicator (Qsonica, Newtown, CT, USA) equipped with a 3 mm probe (maximum amplitude 180 μm). Emulsions were homogenized at an amplitude of 75 %, running 2 passes of 30 s with a break of 1 min between passes. An SDS-stabilized O/W emulsion was also prepared under the same conditions as described above. This emulsion and its dilutions were used for SRCD baseline correction. Five hundred microliters of each emulsion were centrifuged at 13,500 rpm for 30 min (Eppendorf Minispin®, Eppendorf Nordic, Denmark) to separate the resulting bottom phase (aqueous phase) from the top phase (oil phase). The oil phase was later re-suspended, with buffer addition of the same amount as the original aqueous phase removed. This was carried out to separate the excess hydrolysate in the aqueous phase, which allowed the CD signal to be obtained from only the peptides located at the O/W interface. The re-suspended oil phase, untreated emulsion, and aqueous phase were further diluted in buffer (1:4, 1:22, and 1:22 v/v) to adjust the maximum absorbance measured. The whole process of preparing and measuring all the different solutions described above was accomplished within 2.5 days and carried out in duplicate. Temperature scans were carried out for re-suspended oil phases obtained from emulsions stabilized with GT and BT hydrolysates, and SRCD measurements were taken at temperatures from 5.7 $^{\circ}\text{C}$ to 84.5 $^{\circ}\text{C}$ in steps of 5 °C, recorded in triplicate at each step.

2.5.2. Interfacial adsorption and dilatational rheology

Interfacial tension (adsorption) and dilatational rheology quantification were carried out according to Pérez-Gálvez et al. (2024) [15] and Ruiz-Álvarez et al. (2022) [44], with slight modifications. The experiment was performed in a pendant drop (PD) tensiometer designed at the University of Granada (patent ES 2 153 296 B1/WO 2012/080536 A, ES), which operates with DINATEN® and CONTACTO® Software (both developed at the University of Granada). The PD tensiometer is described elsewhere [45].

The experiment is fully computer-controlled by DINATEN® Soft-

ware, which also records the interfacial tension response to the area deformation and calculates the drop volume (V, μL), the interface area (A, mm^2), and interfacial tension (IFT, mN/m) based on Axisymmetric Drop Shape Analysis (ADSA) of the digitalized pendant drop images, adjusting to the Young-Laplace equation of capillarity (Maldonado-Valderrama et al., 2015; Ruiz-Álvarez et al., 2022). Based on DINATEN© outputs, CONTACTO© Software calculates the complex dilatational modulus (E) and related quantities (storage (E') and loss (E'') modulus), given in the general case by Eq. (6).

$$E = E' + i E'' = (\varepsilon_d) + (i f \eta_d)$$
(6)

where: E' is equal to interfacial dilatational elasticity (ϵ_d), the interfacial layer property to resist deformation and restore initial interfacial tension after stress; E'' is proportional to dilatational interfacial viscosity (η_d) and oscillatory angular frequency (f). The interfacial dilatational viscosity measures the speed of the relaxation process to restore the equilibrium after the disturbance, representing the ability of the interfacial layer to adapt to a deformation [47].

In the present work, an aqueous solution of each of the six hydrolysates (GS, GT, WS, WT, BS, and BT) at concentration of 0.1 g protein/L was prepared in ultrapure water. The pH solution was adjusted to 7 by 0.2 M NaOH addition. The solution remained under stirring overnight at 4 °C, and the pH was confirmed and adjusted, if needed, before the analysis. The aqueous solutions were prepared in duplicate, and time was given to reach the temperature of 25 °C. The initial droplet volume and interfacial area were set to 30 μL and 45 mm², respectively. Drops were formed directly into echium oil contained in a thermostated cuvette. The IFT of the bare echium oil-water interface was checked prior each experiment providing values of 25.0 \pm 0.5 mN/m.

After equilibration of the interfacial layer, the droplet was subjected to sequential area deformation with varying frequency (linear rheology) and amplitude (nonlinear rheology). At linear rheology, the initial interfacial area deformation ([A - $A_0]$ / A_0) was kept at 5 % while the frequency of the periodic deformation varied as follows: 0.01, 0.02, 0.05, 0.1, 0.2, 0.4 Hz. At non-linear rheology, the oscillating frequency was maintained constant at 0.02 Hz and the initial interfacial area deformation was set to 5, 10, 20, and 30 %. All measurements were at least in duplicate.

2.6. Production of emulsions and sampling

Six different emulsions containing 5 % wt. of echium oil and stabilized with each hydrolysate (GS, GT, WS, WT, BS, and BT) were produced, according to Padial-Domínguez (2020) [47]. In brief, each hydrolysate was solubilized in milli-Q water (2 % wt. of protein) and stirred overnight at 4 °C to completely rehydrate the protein. Then, a 10 % sodium-azide aqueous solution was added to the aqueous phase to a final concentration in the coarse emulsion of 0.05 % (v/w), and the pH was adjusted to 7.0 by 0.2 M NaOH addition. A pre-emulsion process (3 min at 15,000 rpm) was carried out in an Ultra-turrax T-25 homogenizer (IKA, Staufen, Germany), with the oil phase (echium oil, 5 %, w/w) dispersed in the aqueous phase in the first minute. The coarse emulsions were homogenized in two stages high-pressure homogenizer (Panda PLUS 2000, GEA Niro Soavi, Lübeck, Germany) at 450/75 bar, applying 3 passes. Finally, to accelerate the oxidation, FeSO₄ aqueous solution was added to the emulsion at a final concentration of 100 μM of ferrous ions (Fe²⁺). Twenty-five milliliters of emulsion were poured into 50 mL amber glass bottles and stored at 25 °C for 7 days. Samples were taken on days 0, 2, 5, and 7 for emulsion physical and oxidative stability analysis. For the latter, the bottle atmosphere was then saturated with nitrogen gas and conserved at $-80\,^{\circ}\text{C}$ until the analysis was carried out. The ζ -potential was determined on day 1.

2.7. Physical stability of emulsions

2.7.1. ζ-Potential

The net electrical surface charge of droplets in each emulsion was measured on day 1 of storage in a Zetasizer Nano ZS (Malvern Instruments Ltd., Worcestershire, UK) fitted with DTS-1070 disposable capillary cell (Malvern Instruments, Ltd., United Kingdom). The emulsions were diluted (1:10) in distilled water and 1 mL was introduced into the capillary cell to analyze the ζ -potential, which was set to -100 to +50 mV, and the samples were analyzed with 100 runs. The particle refractive index, particle absorption index, and dispersant refractive index were 1.45, 0.001, and 1.33, respectively. Measurements were carried out in triplicate.

2.7.2. Droplet size and size distribution

The droplet size and size distribution were measured by laser diffraction in a Malvern Mastersizer 3000 equipment (Malvern Instruments Ltd., Worcestershire, UK) [47]. The emulsions were directly diluted in distilled water under recirculation (3000 rpm) until obscuration of $10{\text -}15$ %. The refractive index was 1.481 for the dispersed phase (echium oil) and 1.330 for the dispersant (distilled water). Measurements were carried out in triplicate and results were expressed as volume mean diameter (D_{4,3}) (Eq. (7)), Sauter mean diameter (D_{3,2}) (Eq. (8)), percentile 90 (D₉₀).

$$D_{(4,3)} = \sum n_i d_i^4 / \sum n_i d_i^3$$
 (7)

$$D_{(3,2)} = \sum n_i d_i^3 / \sum n_i d_i^2$$
 (8)

where n represents the number of droplets with a specific diameter, d is the diameter of the droplet, and i represents the size class of the droplets.

2.7.3. Creaming index

On day of preparation (0), all emulsions were filled into graduate creaming tubes to allow measuring of the creaming rate on 0, 2, 5, and 7 days of storage at 25 $^{\circ}$ C. The creaming index (CI) was calculated as described by Eq. (9).

$$CI\left(\%\right) = \frac{H}{Ho} \times 100\tag{9}$$

where H is the height of aqueous phase separated at the bottom of the graduated cylindrical tube, and Ho is total height of emulsion in the tube.

2.7.4. Multiple light scattering measurement

The physical stability of emulsions was further evaluated by multiple light scattering measurement in an optical analyzer Turbiscan LAB (Formulaction, Toulouse, France), as previously described by Ospina-Quiroga et al. (2024) [48]. To this end, 20 mL of each emulsion, without any dilution, were poured into a flat-bottomed glass cylindrical cell. Then, a mobile reading head, composed of a near infrared light-emitter and two detectors (transmission (T) and backscattering (BS)), scanned the glass cell containing the sample along its heigh, plotting BS against height and time and calculating the Turbiscan Stability Index (TSI). The BS is affected by particle migration (creaming, sedimentation) and particle size variation (coalescence, flocculation) [49]. The Turbiscan Stability Index (TSI) value is an average of all processes taking place in the sample (thickness of sediment and clear layer, process of particles settling) [50]. The experiment was repeated at days 0, 2, 5, and 7 of storage.

2.8. Oxidative stability of emulsions

2.8.1. Peroxide value (PV)

Five hundred milligrams of emulsion were added to 20 mL of 2-

propanol/hexane (1:1, v/v) and mixed for 5 min to extract the echium oil. The solution was centrifuged at 670 $\times g$ for 2 min (Hermle D-78564, Hermle Labortechnik GmbH, Germany), and the upper phase was poured into a 10 mL Pyrex glass tube to be dried under nitrogen gas flow. The extracted oil was resuspended in 10 mL of 2-propanol, from which 3 mL were transferred to three other Pyrex tubes, one to determine the mass of oil extracted by gravimetry and two for carrying out oxidation analyses. Hydroperoxide content was determined on the lipid extracts using the colorimetric ferric-thiocyanate method as described by Shantha and Decker (1994) [51]. The absorbance was measured at 485 nm in a Genesys 30 visible spectrophotometer (Thermo Fisher Scientific). The lipid extraction was performed in duplicate, and the peroxides measurement was carried out in quadruplicate. Results were expressed as $m_{\rm eq}$ O_2/kg oil.

2.8.2. p-Anisidine value (p-AV)

Secondary oxidation products (aldehydes) were quantified by p-AV analysis, as described by the ISO method [52]. Extracted oil (\sim 150 mg) was mixed with hexane, vortexed, and separated into two equal volumes. The first volume was mixed with p-anisidine dissolution in acetic acid, whereas the second volume was employed as the control. All of them were covered and left in the dark for 10 min before measuring absorbance at 350 nm. The results are expressed as a 100-fold increase in absorbance of a test solution that was reacted with anisidine at certain conditions stipulated by the ISO method.

2.9. Statistical analysis

Statistical data analysis was conducted on GraphPad Prism version 10.3.0 for Windows (GraphPad Software, Boston, MA, USA). Data normality was evaluated by the Shapiro Wilk test. According to normality test, to compare time-dependent changes inside each group of emulsion, repeated measure (RM) one-way ANOVA or Friedman test was performed followed by Tukey test or Dunn's multiple comparison test, respectively. To compare hydrolysate effects among groups of same enzymatic treatment and time, one-way ANOVA or Kruskal-Wallis test, followed by Tukey test or Dunn's post hoc testing was used. To compare the effect of enzymatic treatment at the same raw material and days of storage, paired t-test or Wilcoxon test was performed. Data were expressed as the mean \pm standard deviation and the significant level was set at p-value of 0.05.

3. Results and discussion

3.1. Enzymatic hydrolysis and characterization of hydrolysates

3.1.1. Enzymatic hydrolysis

Activity of endogenous enzymes was confirmed in all raw materials, although in lower intensity in spent grains derived from whiskey production. Thus, various time and temperature conditions were tested for thermal inactivation of these endogenous enzymes, resulting in effective slowing down of the proteolytic activity of the present enzymes under the conditions of 90 °C for 15 min (Supplementary material, Fig. S.1). Thus, carrying out the thermal deactivation would imply that the release of peptides from the starting protein material is only because of the exogenous enzymes added. Serine endopeptidases, such as subtilisin (EC.3.4.21.14) and trypsin (EC.4.21.4), are among the most used proteases to produce emulsifying and antioxidant peptides from both animal and plant derived raw materials [15,18,33,53,54]. On the one hand, Alcalase is a commercial enzyme preparation from Bacillus licheniformis, made mainly of subtilisin A, an endopeptidase with broad spectrum of action that preferably cleaves terminal hydrophobic amino acids [17]. On the other hand, trypsin is a highly specific protease that exclusively cleaves C-terminal to arginine or lysine [55]. Therefore, the enzyme cleavage specificity and the type of side stream material, which determines the type of peptide bonds available, play a crucial role in the

hydrolysis yield and characteristics of the hydrolysate.

The efficiency of the enzymatic treatment was described in terms of total solids recovery and protein recovery (Table 1). Before the hydrolysis, the protein content of the raw materials agreed with those previously reported in the literature, ranging from 12.1 \pm 1.1 wt% for grape seed flour to 18.9 \pm 0.3 wt% for brewer's spent grains. Spent grains obtained from whisky production showed a slightly lower protein content (11.5 \pm 0.2 wt%) than previously reported. The main proteins in barley spent grains are hordeins (35-55 %, high molecular weight) and glutelin (23 %, low molecular weight), exhibiting great emulsifying properties [23,56]. However, protein extractability depends on the brewing process steps since protein and carbohydrate complexes may be formed during the mashing process [23]. Moreover, during the malting process, barley proteins are partially degraded into amino acids and small peptides by several endogenous proteases [57]. Hence, the low protein content of spent grains from whisky production may be related to these processes, that previously extracted or denatured barley proteins. These processes may also explain why, at the same hydrolysis conditions in comparison to brewer's spent grains, the hydrolysis of spent grains from whisky presented the highest total solids recovery and protein solubilization, without increasing the protein content in the WS and WT hydrolysates (11.4 % and 11.5 %, respectively) comparing to the starting material. As a result, it may be the underlying reason for further differences between W and B hydrolysates regarding emulsifying capacity as indicated in the subsequent sections. Grape seed proteins are mainly composed of 11S and 7S globulins, storage proteins of large molecular weight, also presenting functional properties, such as good solubility and emulsifying capacity [58]. In the present study, enzymatic treatments could poorly (<5 %) recover solids from defatted grape seed flour (G) (Table 1). However, the hydrolysates obtained (GS and GT) presented an increased protein content in comparison to the original protein content of the flour.

Among the six hydrolysates, BS and BT had highest protein content

(36.9–39.6 wt%), followed by the grape seed hydrolysates (26.2–27.2 wt%) and the whisky hydrolysates (11.5 wt%) (Table 1). Interestingly, no marked differences were observed in the protein recovery and protein content of the hydrolysates between the two enzymatic treatments assayed (subtilising or trypsin), except for WS which showed a considerably higher solids and thus protein solubilization when compared to WT (Table 1). In any case, it should be noted that the limited DH (5 %) resulted into a lower protein recovery than other plant materials hydrolysates (such as sunflower and olive seed flours) at 20 % of DH [48]. Although protein content could be increased by further hydrolysis of the starting materials, the DH of 5 % was choose since it has been previously reported to improve the emulsifying activity of the hydrolysates [33,48].

3.1.2. Molecular weight distribution

The progress of enzymatic hydrolysis (measured by DH) as well as the total solids and protein recovery are intrinsically correlated to the molecular weight (MW) distribution of the hydrolysates. Fig. 1 shows the MW distribution of the hydrolysates split into five categories (fractions >7 kDa, 5–7 kDa, 3–5 kDa, 1–3 kDa, and 0.1–1 kDa). The original chromatograms are shown in the Supplementary material (Fig. S.2). BS and BT hydrolysates presented the highest proportion of large molecular weight compounds (fractions 3–5 kDa, 5–7 kDa, and superior to 7 kDa). Intermediate peptides (1 to 3 kDa) were prevalent in WS and WT hydrolysates. Finally, GS and GT had a higher content of short peptides (from 0.1 to 1 kDa) (Fig. 1), which may be related to the low total solids recovery (<5 %) in the hydrolysis of G (Table 1), since just short peptides were extracted from the original raw material, or the larger released peptides were further hydrolyzed once in solution by the enzymes.

Compared to parent proteins, peptides present smaller sizes, and their hydrophobic and polar groups are more exposed, which helps to increase aqueous solubility, diffusivity, and amphiphilic potential [59]. In addition, the molecular size, amino acid sequence, and composition

Table 1
Solids and protein recovery of the enzymatic processes and protein content and amino acid composition of the hydrolysates.

	G	GS	GT	W	WS	WT	В	BS	BT
Total solids recovery (%)	_	$4.1\pm0.2^{\rm e}$	4.7 ± 0.1^{d}	_	27.4 ± 0.1^a	$19.9\pm0.1^{\rm b}$	_	$8.3\pm0.2^{\rm c}$	$8.3\pm0.3^{\rm c}$
Protein recovery (%)	_	$9.0\pm0.4^{\rm f}$	$10.3\pm0.1^{\rm e}$	_	27.2 ± 0.1^a	$19.8\pm0.1^{\rm b}$	_	$17.4\pm0.5^{\rm c}$	$16.2\pm0.6^{\rm d}$
Protein content (g/100 g)	$12.1\pm1.1^{\rm e}$	26.2 ± 0.2^{c}	$27.2\pm0.3^{\rm c}$	$11.5\pm0.2^{\rm e}$	$11.4\pm0.2^{\rm e}$	$11.5\pm0.2^{\rm e}$	$18.9 \pm 0.3^{\text{d}}$	39.6 ± 0.1^a	$36.9\pm0.2^{\rm b}$
Isoelectric point (mV)	_	1.39 ± 0.2^{d}	1.77 ± 0.0^{c}	-	3.12 ± 0.0^a	1.39 ± 0.1^a	_	2.75 ± 0.1^{b}	2.84 ± 0.0^{b}
Amino acid (% molar)									
His	2.3 ± 0.0^a	$1.3\pm0.0^{\rm h}$	$1.4\pm0.0^{\rm g}$	$2.2\pm0.0^{\rm b}$	$2.1\pm0.0^{\rm c,d}$	$2.0\pm0.0^{\rm e}$	$2.1\pm0.0^{\mathrm{b,c}}$	$2.0\pm0.0^{\rm d}$	$1.8\pm0.0^{\rm f}$
Ile	$2.5\pm0.2^{\rm e}$	$2.4\pm0.1^{\rm e}$	$4.0\pm0.0^{\mathrm{b,c}}$	$4.0\pm0.0^{\mathrm{b,c}}$	$3.6\pm0.1^{\rm d}$	3.9 ± 0.0^{c}	$4.1\pm0.0^{\rm b}$	4.3 ± 0.0^a	$4.1\pm0.0^{\rm b}$
Leu	$5.0\pm0.2^{\rm h}$	$5.3\pm0.0^{\rm g}$	$5.9\pm0.0^{\rm f}$	7.8 ± 0.1^{c}	$6.8\pm0.1^{\rm e}$	$7.3\pm0.0^{\rm d}$	10.7 ± 0.0^a	$7.6\pm0.0^{\rm c}$	$8.2\pm0.0^{\rm b}$
Lys	$3.3\pm0.1^{b,c}$	$1.4\pm0.0^{\rm f}$	$1.9\pm0.0^{\rm e}$	4.4 ± 0.4^a	$3.6\pm0.1^{\rm b}$	$3.1\pm0.0^{\mathrm{c,d}}$	$3.1\pm0.1^{\rm c,d}$	4.1 ± 0.0^a	$2.8\pm0.0^{\rm d}$
Met	$1.0\pm0.1^{\rm d}$	$0.9 \pm 0.0^{\rm d}$	$1.0\pm0.0^{\rm d}$	$1.3\pm0.1^{\rm c}$	$1.7\pm0.0^{\rm b}$	$1.7\pm0.0^{\rm b}$	$1.3\pm0.1^{\rm c}$	1.9 ± 0.0^a	$1.7\pm0.0^{\rm b}$
Cys	1.1 ± 0.0^a	1.1 ± 0.1^a	$0.8\pm0.0^{\mathrm{b}}$	0.6 ± 0.0^{c}	1.1 ± 0.0^a	$0.6\pm0.1^{\mathrm{b,c}}$	$0.6\pm0.1^{\rm c}$	1.1 ± 0.0^a	1.1 ± 0.0^a
Phe	2.6 ± 0.0^d	$3.8\pm0.2^{\rm c}$	$3.7\pm0.1^{\rm c}$	$4.3\pm0.1^{\rm b}$	$3.7\pm0.1^{\rm c}$	$4.2\pm0.0^{\mathrm{b}}$	4.7 ± 0.0^a	$4.3\pm0.1^{\rm b}$	4.7 ± 0.0^a
Tyr	$1.7\pm0.2^{c,d}$	$2.1\pm0.0^{\rm b,c}$	$2.3\pm0.1^{\rm b}$	$0.9\pm0.2^{\rm f}$	$1.6\pm0.3^{\rm d,e}$	$1.6\pm0.1^{\rm d,e}$	$1.1\pm0.2^{\rm e,f}$	3.1 ± 0.0^{a}	2.9 ± 0.1^a
Thr	$3.8\pm0.0^{\rm f}$	$3.0\pm0.1^{\rm h}$	$3.3\pm0.0^{\rm g}$	4.9 ± 0.1^a	4.9 ± 0.0^a	4.4 ± 0.0^{c}	$4.3\pm0.0^{\rm d}$	$4.6\pm0.0^{\rm b}$	$4.0\pm0.0^{\rm e}$
Val	$4.5\pm0.1^{\rm g}$	$4.9 \pm 0.0^{\rm f}$	$6.2\pm0.0^{\rm d}$	7.2 ± 0.1^a	7.2 ± 0.0^a	$6.9\pm0.0^{\rm b}$	$6.1\pm0.1^{ m d,e}$	$6.5\pm0.1^{\rm c}$	$5.9\pm0.0^{\rm e}$
Asp	$9.1\pm0.3^{\rm b,c}$	10.5 ± 0.0^a	$9.5\pm0.0^{\rm b}$	$9.0\pm0.3^{\rm c}$	$9.1\pm0.0^{\rm b,c}$	$8.2\pm0.0^{\rm d}$	$7.0\pm0.1^{\rm e}$	$8.5\pm0.0^{\rm d}$	$7.0\pm0.1^{\rm e}$
Glu	22.6 ± 0.7^{c}	29.4 ± 0.0^a	$26.2\pm0.0^{\rm b}$	$14.9\pm0.7^{\rm g}$	$15.9\pm0.2^{\rm f,g}$	$18.2\pm0.0^{\rm e}$	$17.9\pm0.1^{\rm e}$	$16.3\pm0.0^{\rm f}$	20.6 ± 0.0^{d}
Ser	$6.9\pm0.1^{a,b}$	$6.8\pm0.0^{\rm b,c}$	7.1 ± 0.0^a	$6.9\pm0.1^{b,c}$	$6.8\pm0.1^{\rm b,c}$	$6.3\pm0.0^{\rm d}$	$6.7\pm0.0^{\rm c}$	$6.2\pm0.0^{\rm d}$	$6.0\pm0.0^{\rm e}$
Arg	4.3 ± 0.2^a	$2.2\pm0.0^{\rm d}$	$3.4\pm0.0^{\rm b}$	$2.8\pm0.1^{\rm c}$	$3.0\pm0.3^{\rm b,c}$	2.7 ± 0.0^{c}	$2.1\pm0.2^{\rm d}$	4.2 ± 0.0^a	$3.1\pm0.0^{\rm b,c}$
Ala	$7.5\pm0.1^{\rm d}$	$7.1\pm0.0^{\rm d,e}$	$6.8\pm0.0^{\rm e}$	9.8 ± 0.4^a	9.8 ± 0.1^a	$8.9\pm0.0^{\rm b}$	9.8 ± 0.2^a	$8.1\pm0.0^{\rm c}$	$7.6\pm0.0^{\rm d}$
Pro	4.6 ± 0.2^{e}	4.6 ± 0.0^{e}	4.8 ± 0.1^{e}	$9.7\pm0.5^{c,d}$	$9.9\pm0.0^{\rm c}$	$11.6\pm0.0^{\mathrm{a,b}}$	$11.3\pm0.1^{\rm b}$	$9.3\pm0.0^{\rm d}$	11.9 ± 0.0^a
Gly	17.1 ± 0.1^a	$13.1\pm0.0^{\rm b}$	11.8 ± 0.0^{c}	9.4 ± 0.2^{d}	9.3 ± 0.1^{d}	8.4 ± 0.0^e	7.1 ± 0.2^g	$7.8\pm0.0^{\rm f}$	$6.5\pm0.0^{\rm h}$
Distribution of amino acids (% molar)									
Hydrophobic*	$27.8 \pm 0.7^{\rm f}$	$29.2\pm0.3^{\rm e}$	$32.4\pm0.1^{\rm d}$	$44.1\pm0.1^{\rm b}$	42.7 ± 0.1^{c}	$44.5\pm0.1^{\rm b}$	48.0 ± 0.0^a	42.2 ± 0.1^{c}	$44.2\pm0.0^{\rm b}$
Hydrophilic**	$41.7\pm0.7^{\rm b}$	44.8 ± 0.1^a	$42.4\pm0.0^{\rm b}$	$33.2\pm0.1^{\text{e}}$	$33.6\pm0.1^{d,e}$	34.2 ± 0.0^{d}	$32.3\pm0.1^{\rm f}$	$35.1\pm0.1^{\rm c}$	$35.3\pm0.0^{\rm c}$
Neutral***	30.4 ± 0.0^a	$26.1\pm0.1^{\rm b}$	25.2 ± 0.1^{c}	22.7 ± 0.1^e	23.7 ± 0.2^{d}	$21.4\pm0.1^{\rm f}$	$19.8\pm0.1^{\text{h}}$	22.7 ± 0.0^e	$20.5\pm0.0^{\rm g}$

Abbreviations: (–) not applicable/determined; G: defatted grape seed flour; W: barley spent grains from whisky production, B: barley spent grains from beer production; GS, WS, BS: G, W, and B hydrolysate obtained from subtilisin, respectively; GT, WT, BT: G, W, and B hydrolysate obtained from trypsin, respectively; *Hydrophobic (Ala, Val, Met, Phe, Leu, Ile, Pro); *Hydrophobic (Arg, Asp, His, Lys, Glu); ***Neutral (Ser, Gly, Thr, Tyr, Cys) Values are means \pm standard deviations of three measurements. Different small letters at the same raw present difference at significant level of p < 0.05 by one-way ANOVA and Tukey test.

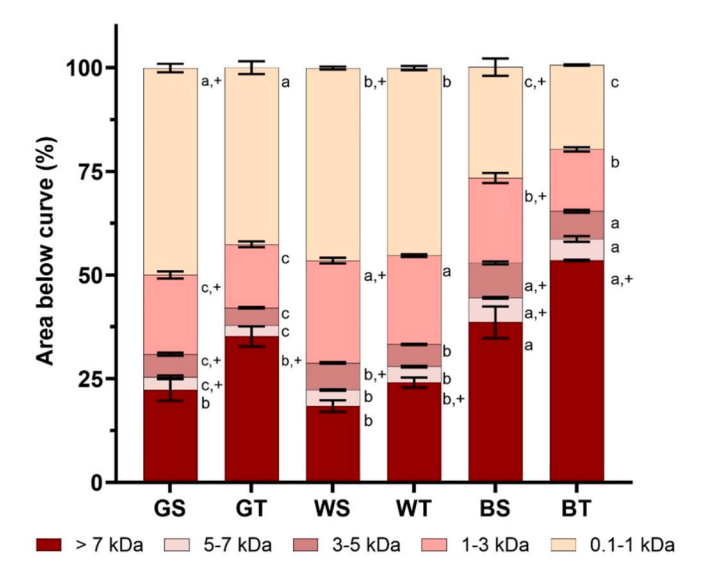


Fig. 1. Molecular weight distribution (percentage area under the curve) of hydrolysates. Sample's code first letter refers to the original side-stream material (defatted grape seed flour (G), barley spent grains from whisky production (W) and barley spent grains from beer production (B)), followed by enzymatic treatment (hydrolysis with subtilisin (S) or trypsin (T)). Different small letters indicate difference among hydrolysates obtained from the same enzymatic treatment according to one-way ANOVA and Tukey post-hoc test (p < 0.05). (+) Indicates differences between enzymatic treatment at the same original side-stream product by unpaired t-test (p < 0.05).

— particularly the presence of hydrophobic amino acids such as His, Met, Cys, Pro, Val, Phe, Tyr, and Trp — have been reported to play an important role in the antioxidant capacity of peptides. This capacity can be exerted through different mechanisms, such as stabilizing free radicals by electron donation or chelating metal ions [33]. Since free radicals and metal ions are reactive species that can initiate the lipid oxidation cascade, antioxidants with the capacity to act through these mechanisms are essential for providing oxidative stability to emulsions. Particularly, the location of the antioxidants at the oil-water interface, where peptides adsorb and unfold, is of special relevance since this is the place where lipid oxidation begins in emulsions [13,15,33].

Large peptides, containing significant hydrophobic patches, can appropriately unfold at the O/W interface providing steric hindrance and electrostatic repulsion [33,60]. In this regard, the enzymatic treatment with trypsin is more interesting since it generates higher content of large peptides (MW superior to 7 kDa) in comparison to subtilisin hydrolysis. It is a consequence of the high selectivity of trypsin, which cleaves a considerably limited type of peptide bonds when compared to subtilisin. Similar results were previously obtained for other plant-based substrates such as olive meal [15]. Previous studies have reported the marked influence of the molecular weight of peptides on their emulsifying activity, with hydrolysates produced at low DH (limited hydrolysis) showing higher emulsifying activity [33,61]. For instance, chickpea protein hydrolysate obtained with Alcalase (1:1 U/mg E/S) showed high emulsifying capacity when obtained at DH of 4 %, and soy protein isolated hydrolyzed with trypsin (0.5 % E/S) at DH of 6 % [47,62]. Moreover, sunflower and olive seed meals were hydrolyzed with trypsin or subtilisin (E/S 0.5 %) at DH of 5 % and pH of 7 or 4 showing improved emulsifying properties of the hydrolysates produced at DH 5 %, pH 7 with trypsin [15].

3.1.3. Amino acid composition and in vitro antioxidant capacity

Subtilisin-derived hydrolysates containing low MW peptides (obtained by hydrolysis at high DH) have been reported to show high antioxidant capacity [17,53]. In fact, peptides with nucleophilic sulphur-containing amino acids (Cys and Met), aromatic ring (Tyr, and

Phe), imidazole-ring (His), indole and pyrrolidine ring (Trp and Pro), basic (Lys, Arg), and hydrophobic amino acid may promote antioxidant capacity by scavenging radicals and hydrogen donation to electron-deficient radicals [53,63].

Table 1 shows the amino acid composition of the starting plant-based materials, and the hydrolysates obtained. The enzymatic treatment changed the composition of some amino acids in the hydrolysates in comparison to starting materials (Table 1). Grape seed flour and barley spent grains from whisky and beer production presented similar amino acid composition to the previous content describe in the literature [27,64]. However, it is worth noting that >40 % of WS, WT, BS, and BT amino acids were hydrophobic. Regarding the antioxidant amino acids described above, Cys and Met increased in the hydrolysates WS and BS and were maintained in GS, compared to the raw materials. Nonetheless, Phe was reduced in WS and BS hydrolysates and increased in GS. Moreover, Tyr increased in the six hydrolysates, while the three original raw materials had higher amounts of His than the six hydrolysates. Trypsin hydrolysis increased Pro content in WT and BT while subtilisin increase the content of Lys in WS and BS. Both amino acids (Pro and Lys) content was reduced in GS, GT in comparison to G.

In vitro screening tests are cost-efficient assays to investigate the antioxidant capacity of new compounds. The six hydrolysates were analyzed according to their ability to scavenge DPPH radicals and chelate metal ions (e.g. ${\rm Fe}^{+2}$) (Fig. 2). The GS and GT hydrolysates showed the highest antioxidant capacity based on their lowest IC₅₀ for both antioxidant mechanisms. Interestingly, although W and B were barley spent grains, WS and WT hydrolysates presented higher DPPH radical scavenging capacity. On the contrary, BS and BT were more effective in the iron chelating mechanism. In addition, it was observed that the enzymatic treatment influenced the antioxidant capacity of hydrolysates. For instance, GS and BS showed higher DPPH radical scavenging capacity. On the other hand, GT and BT presented higher iron chelating activity. Conversely, subtilisin hydrolysis of W has shown increased iron chelating activity in comparison to trypsin hydrolysis, with no difference in the DPPH radical scavenging capacity.

There is no consensus in the literature whether hydrolysates with higher antioxidant capacity are generated by low or high DH. However, peptides with hydrophobic amino acids such as His, Met, Cys, Pro, Val, Phe, Tyr and Trp are describe as antioxidants by DPPH scavenger capacity while peptides with His, Glu, Asp, Lys, and Arg present iron chelating activity [33]. Hence, the antioxidant capacity exhibited by W and B hydrolysates may be related to a higher percentage of hydrophobic amino acids, especially His, Cys, Met, Tyr, Pro, Lys. Likewise, the antioxidant capacity of grape flour seed hydrolysates might be explained by their content in His, Cys, Met, Phe, Tyr, and Arg. Moreover, the higher amount of low molecular weight peptides in GS and GT hydrolysates also might contribute to improve their antioxidant capacity [21,32].

Other compounds than antioxidant peptides may also influence the antioxidant capacity of hydrolysates, such as phenolic compounds. Around 70 % of grape phenolic compounds remain in the solid residue after wine production. Grape seed flour has proanthocyanidins, flavonoids, phenolic acids, and stilbenes [65]. Barley spent grain also has phenolic compounds such as ferulic acid, p-coumaric acid, sinapic acid, and caffeic acids [31,64]. The composition of phenolic compounds was not the focus of our study. Thus, future research may confirm the presence of these minor components in the hydrolysates, which might explain the considerably higher DPPH radical scavenging activity of grape hydrolysates.

3.2. Interfacial properties of hydrolysates

3.2.1. Secondary structure and interfacial conformation of adsorbed hydrolysates

Far-UV circular dichroism is a well-established technique for characterizing the secondary structure of proteins and peptides [14]. It is

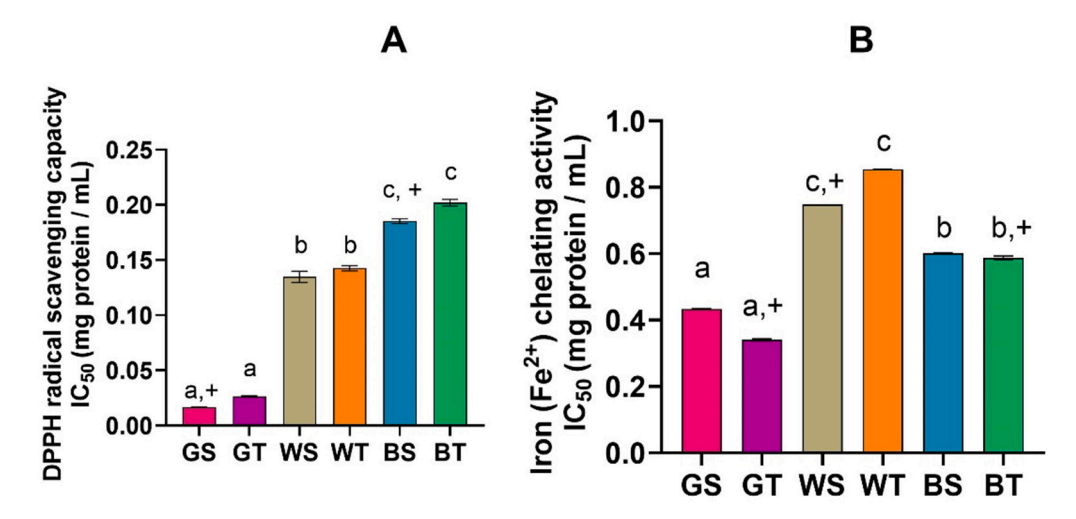


Fig. 2. IC_{50} value for A) DPPH scavenging and B) Iron chelating capacity of all hydrolysates. Sample's code first letter refers to the original side-stream product (defatted grape seed flour (G), barley spent grains from whisky production (W) and barley spent grains from beer production (B), followed by enzymatic treatment (hydrolysis with subtilisin (S) or trypsin (T)). Different small letters indicate difference among hydrolysates obtained from the same enzymatic treatment according to one-way ANOVA and Tukey post-hoc test (p < 0.05). (+) Indicates differences between enzymatic treatment at the same original side-stream product by unpaired *t*-test (p < 0.05).

based on the differential absorption of left or right-handed circularly polarised light, below 240 nm (far-UV), due to the molecule's chiral centre or three-dimensional structure, creating a chiral environment [66]. Therefore, it is interesting to investigate if the adsorption of emulsifying peptides at the O/W interface promotes a conformational change in the peptide structure in order to maximize contact points to the interface, and how this affects the interfacial adsorption and mechanical strength of the interfacial protein film which will determine the physical stability of the stabilized emulsions [14,67,68].

The far-UV SRCD spectra of each hydrolysate in solution (pH $\sim 7)$ shows that peptides dissolved in the aqueous phase present mostly a negative band around 190–200 nm, which characterizes a disordered structure (Fig. 3). However, the reconstituted emulsion (after separation of the solubilized compounds in the aqueous phase of the original emulsion) showed a different CD signal, except for GS and GT (Fig. 3a, b) that did not change their conformation when adsorbed at the O/W interface. Measurements of the centrifuged aqueous phase and diluted emulsions showed no significant difference in CD spectra compared to the solutions (Supplementary material Fig. S.5).

The folding and unfolding of proteins depend on the number and distribution of disulphide bonds, the flexibility of the chains, and the distribution and exposure of hydrophobic regions. Upon adsorption, at the O/W interface the peptides may adopt a new secondary structure, including changes in β -sheet and α -helix content [14]. On one hand, peptides present in WS and WT showed a maximum positive tending CD signal near 190 nm and minimum negative signals at 208 and 222 nm when adsorbed at the O/W interface, which is an indicative of an increase in α -helical structure (Fig. 3c, d) [69]. On the other hand, BS and BT reconstituted emulsions present an increase in β-sheet structure, characterized by a negative elliptic signal at 217 nm (Fig. 3e, f) and the positive tending band at ~190 nm. In this matter, the balance between hydrophilic and hydrophobic amino acids makes the peptide chains to be oriented above and below the plane of the β -strand [14,15]. The secondary structure composition of barley protein concentrates was reported to be variable depending on the type of protein extraction methods [70]. When analyzed by Fourier transformation infrared spectroscopy (FTIR), a barley protein concentrated obtained by alkaline extraction followed by enzymatic carbohydrates hydrolysis, presented most of the α -helix secondary structure, due to the enriched content of globulins and D hordeins, and lower amount of B hordeins and serpins. In addition, barley protein concentrated obtained by alkaline extraction and isoelectric precipitation showed 45 % of β -turns and 25 % of α -helices [56].

To contribute with hydrolysates characterization regarding their thermal stability once they adsorb at the O/W interface, the far-UV SRCD spectra of the reconstituted emulsions stabilized with GT and BT were recorded at different temperature (from 6 to 85 °C) (Supplementary material Fig. S.6.A and B). The eGT and eBT reconstituted emulsion were stable until approximately 40 and 60 °C respectively, after which the intensity of the spectra decreased while further increasing the temperature. Interestingly, the structure was totally recovered after cooling to room temperature (Fig. S.6.A). Similar results were observed for emulsions stabilized with olive meal hydrolysate, being stable until 40 °C before a heat-induced change to the intensity of the CD signal, being partially reversible after re-cooling to 25 °C [15].

3.2.2. Interfacial adsorption and dilatational rheology

The kinetics of interfacial adsorption of proteins/peptides shows generally three periods: induction, adsorption, and stabilization. Firstly, in the induction period, compounds diffuse from the bulk solution to the interface, producing small changes in the interfacial tension (IFT). Secondly, in the adsorption period, a sharp decrease in IFT is observed as the compound is adsorbed at the interface. Lastly, in the stabilization period, the interface saturates, and conformational rearrangements may occur until a stable IFT value is achieved [16]. In drop tensiometers, the adsorption capacity of peptides depends on their diffusion towards the O/W interface, while the reduction in interfacial tension is more strongly influenced peptide amphiphilicity rather than by their size [67].

Fig. 4 shows the evolution of interfacial tension versus time for all the hydrolysates, where no induction period was observed. GS and GT presented the lowest interfacial activity, poorly reducing the interfacial tension, IFT around 22 mN/m. The lower content of hydrophobic amino acids in these hydrolysates (Table 1) had a negative impact in the amphiphilicity of the peptides, which were not able to adsorb at the O/W interface and reduce IFT. Nevertheless, WS, WT, BS, and BT hydrolysates could adsorb at the O/W interface and reduce IFT, showing potential as emulsifiers (final IFT between 15 and 18 Nm/m) (Fig. 4B). These hydrolysates presented peptides with medium and large MW and almost 40 % hydrophobic amino acids, which contributed to the adsorption and potential unfolding at the O/W interface [16]. BT showed the highest reduction of IFT, which is explained by higher

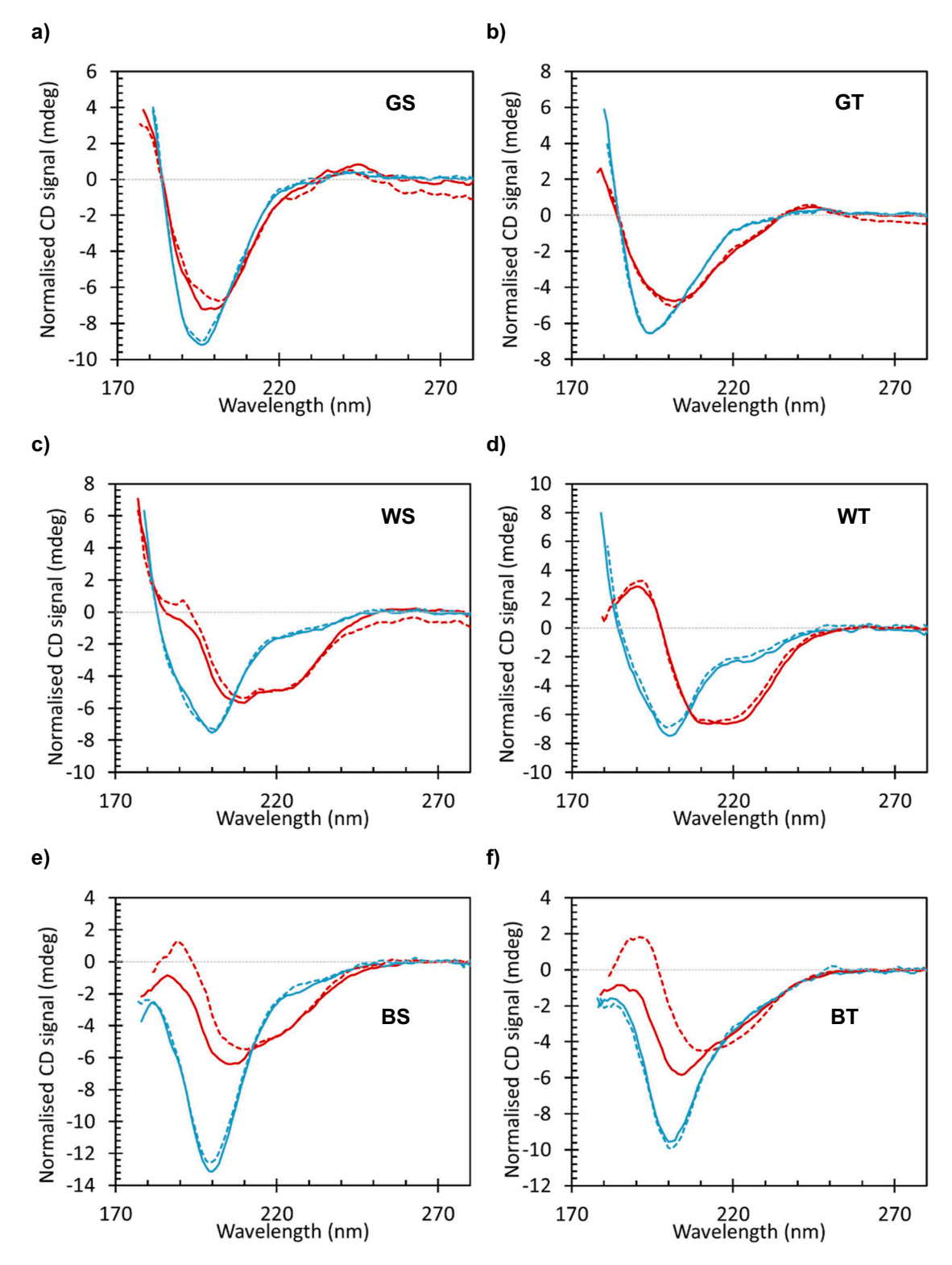


Fig. 3. Far-UV SRCD spectra for solutions (blue lines) and tricaprylin oil-water reconstituted interface (red lines), for replicate A (solid line) and replicate B (dash line). To account for varying concentrations of sample used for measurement (necessary due to the nature of the samples), spectra have been scaled according to the absorbance spectra measured simultaneously with the CD spectra, to better compare the shape and magnitude.

molecular weight of the peptides present in this hydrolysate (Fig. 1), as well as their adequate amphiphilicity because of a high content of hydrophobic amino acids (Table 1), which both favour their adsorption and unfolding at the O/W interface [15].

According to previous study, proteins and polysaccharides complexes formed by electrostatic, hydrogen bonding, hydrophobic, and

non-covalent bonds may affect the interfacial properties due to their effect on adsorption, viscoelasticity, mechanical strength, and electrostatic interactions at the interface [68]. In this regard, protein and carbohydrates interactions, as well as the amino acid content and intermedium MW compounds, might have improved the adsorption capacity of WS and WT hydrolysates to unfold at the interface and

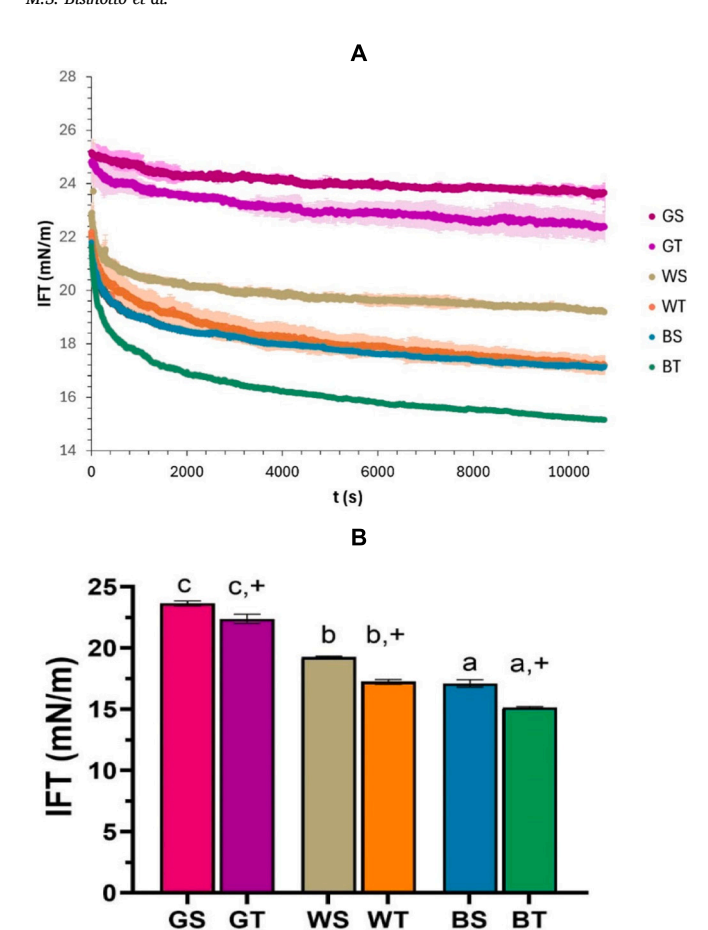


Fig. 4. Interfacial tension (IFT) of hydrolysates solutions: a) as function of time and b) after 3 h adsorption at constant interfacial area. Sample's code first letter refers to the original side-stream product (defatted grape seed flour (G), barley spent grains from whisky production (W) and barley spent grains from beer production (B), followed by enzymatic treatment (hydrolysis with subtilisin (S) or trypsin (T)). Different small letters indicate difference between protein type for the same enzymatic treatment; (+) indicate difference between enzymatic treatment for the same protein type, both at the significance level of p < 0.05.

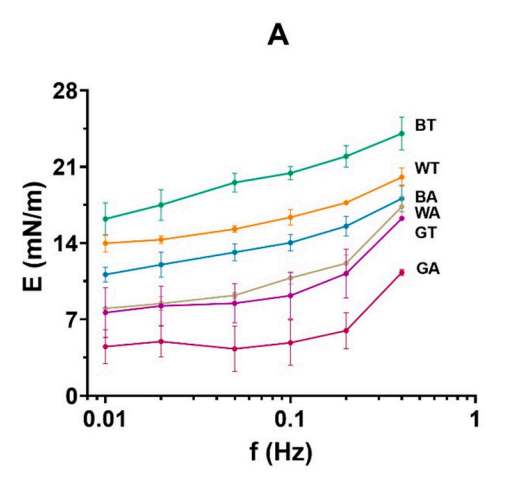
reduce IFT.

Adsorbed peptides at the O/W interface undergo a conformational secondary structure change to unfold at the interface [71], producing viscoelastic films [67]. To evaluate the viscoelasticity of the interfacial peptide film, frequency sweeps (linear rheology) reveal time-dependent deformation behaviour, while amplitude sweeps (nonlinear rheology) describe the response of the interfacial layer, as strength and degree of linearity, to the amplitude of deformation [72]. For all the interfacial films evaluated, the storage modulus (E') was larger than the loss modulus (E") (data not shown), which indicates a predominantly elastic interfacial layer [67]. All interfaces showed a complex modulus inferior to 25 mN/m, which was dependent on frequency (Fig. 5A). It implies short relaxation times suggesting flexible interfacial films [73]. Fig. 5B shows how the complex modulus varied with the amplitude of the applied dilatational deformation (from 5 to 30 %). It was observed that the complex modulus remained nearly constant showing a linear viscoelastic regime, indicating that the increase in amplitude did not affect the interfacial microstructure, implying weak peptides interactions at the O/W interface, leading to easily stretchable interfaces [73]. Nevertheless, it is worth mentioning that the interfacial film formed by the peptides present in the BT hydrolysate showed the highest complex modulus (Fig. 5A, B). This finding could be attributed to the gain in β -sheet structure of these peptides at the interface, which results in more inter-peptide interactions when compared to peptides with more α -helix structure [14,74].

3.3. Physical stability of emulsions

The emulsifying capacity of the hydrolysates was further investigated by their ability to stabilize 5 % echium oil-in-water emulsions. The most critical colloidal interactions for protein-coated oil droplets are van der Waals attraction, hydrophobic attraction, and steric and electric repulsions [75]. To produce physically stable emulsions, the repulsion interactions should be superior to the attraction interactions, as well as no other physical destabilization process, such as gravitational separation (creaming), aggregation (flocculation or coalescence) should take place [75]. It is crucial to note that all emulsions contained a 2%wt. of protein, so consequently, other macro and micro components of plant hydrolysates rather than peptides and proteins (such as carbohydrates and polyphenols) were contained in the emulsions. These compounds may also impact the stability of emulsions.

Emulsion stabilized with GS (eGS) exhibited a monomodal distribution during storage, increasing droplet size from day 0 to day 7



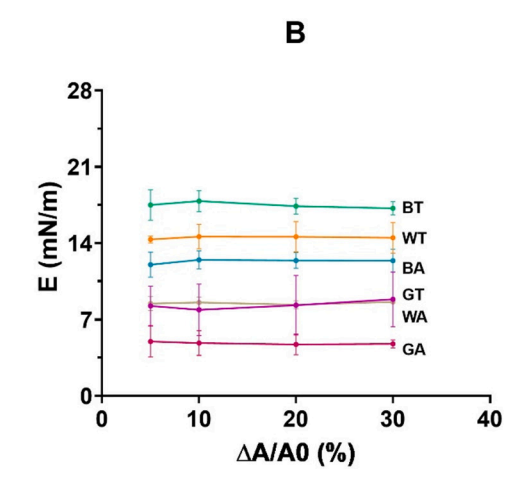


Fig. 5. A) Complex interfacial dilatational modulus (E) of adsorbed layers of hydrolysates as a function of oscillation frequency (f) at 5 % area deformation. B) Complex interfacial dilatational modulus (E) of adsorbed layers of hydrolysates as a function of deformation ($\Delta A/A0$) at oscillation frequency 0.05 Hz. Protein content in all solutions: 0.1 g/L, trycaprilin oil-water interfaces, T = 25 °C. Sample's code first letter refers to the original side-stream product (defatted grape seed flour (G), barley spent grains from whisky production (W) and barley spent grains from beer production (B)), followed by enzymatic treatment (hydrolysis with subtilisin (S) or trypsin (T)).

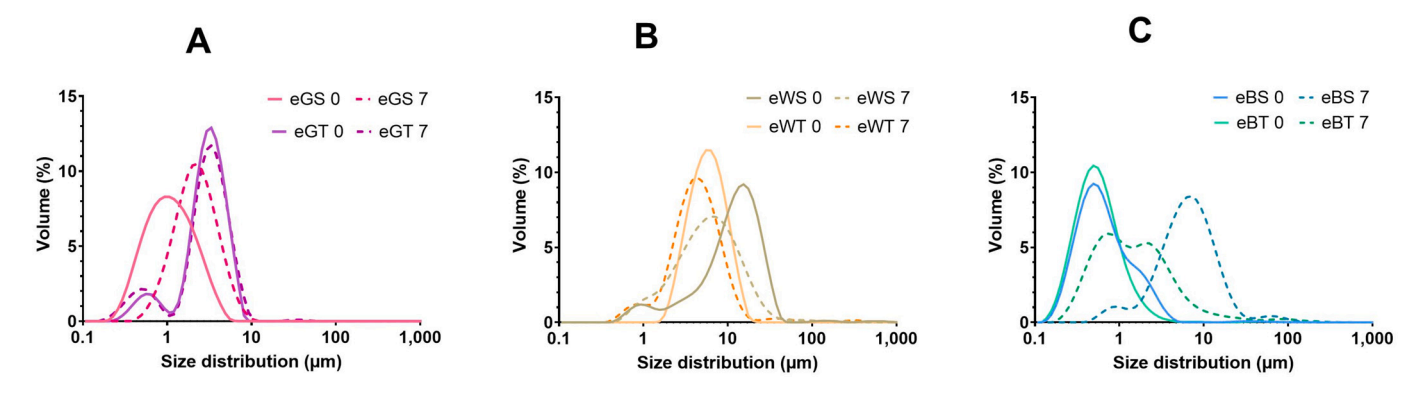


Fig. 6. Droplet size distribution of emulsions at day 0 and 7 of storage. Emulsion's name code means that the first two letters refer to the hydrolysate used to stabilize the emulsion (defatted grape seed flour (eG), barley spent grains from whisky production (eW) and barley spent grains from beer production (eB)), followed by enzymatic treatment applied to the original side-stream product (hydrolysis with subtilisin (S) or trypsin (T)) and day of storage (0 or 7 days).

(Fig. 6A). In contrast, the emulsion stabilized with GT (eGT) showed a bimodal distribution from day 0 without changing the droplet size distribution during storage (Fig. 6A). Although both hydrolysates showed non-organized secondary structure and poorly adsorbed at the O/W interface, the emulsion eGT presented low creaming index (Fig. 7B, and see also Fig. S.4 in Supplementary material) and the highest physical stability given by the lowest TSI (Fig. 7A). The high hydrophilic amino acids content and the majority low MW peptides contributed to poor diffusion of these peptides (GT) from the aqueous phase to the oil interface. Therefore, the energy conferred during the high-pressure homogenization may have contributed to improve diffusion of peptides to the interface during emulsion production and also increase their molecular flexibility and surface hydrophobicity, as described for insoluble soy peptides aggregates [76]. Moreover, tannins from grape were described as surface active compounds developing emulsion stabilization by steric and/or electrostatic repulsions between droplets covered by adsorbed polymers [77].

The emulsions stabilized by WS and BS hydrolysates (eWS and eBS) presented a polydisperse size distribution, while those stabilized by WT and BT hydrolysates (eWT and eBT) showed a monomodal distribution (Fig. 6B, C). After 7 days, the emulsions eWS and eWT presented the highest CI, while eBS, and eBT emulsions presented low destabilization by creaming (Fig. 7B and see also Fig. S.4 in Supplementary material). Our results agree with previous research [23], where the combination of amphiphilic protein and large content of fibres from brewer's spent grains was a double-edged sword. Although sufficient electrostatic repulsion was observed (around $-30 \, \text{mV}$), the presence of fibres resulted in flocculation [23]. It might be the underline reason for eWT developed a worse physical stability in comparison to eGT, despite WT showed

higher content of hydrophobic amino acids content, large MW size peptides and improved interfacial properties.

All emulsions presented a highly negative ζ -potential (lower than -30 mV) on day 1 at pH 7 (Fig. 3), which correlates well with low pI of the hydrolysates (Table 1). Theoretically, this indicates that the electrostatic repulsions created between oil droplets might be high enough to avoid physical destabilization [46]. Nevertheless, the evolution of droplet size (Table 2) and droplet size distribution (Fig. 6) as well as the TSI and CI results (Fig. 7), including Turbiscan backscattering plots (Supplementary material Fig. S.3), revealed physical destabilization of emulsions. Thus, the peptide interfacial layer formed might not present the thickness and strength required to totally prevent droplet flocculation and/or coalescence [67]. In fact, according to dilatational rheology results, the hydrolysates produced weak interfaces (e.g., complex dilatation and modulus lower than 35 mN/m) [14].

In any case, it should be noted that the most physically stable emulsion during storage was eBT, with the lowest $D_{[3;2]}$ and $D_{[4;3]}$ during storage, which leads to small droplet size and hence higher interfacial area (Table 2). This finding agrees with the high adsorption capacity to the O/W interface of this BT hydrolysate (lowest final IFT, Fig. 4) and an interfacial layer more resistance (highest complex modulus, Fig. 5) [78]. These features are intrinsically correlated to the high hydrophobic amino acids content and high percentage of high MW peptides, that boost the peptide's adsorption and their interactions at the interface [15]. In fact, the BT peptides gained in β -sheet structure when adsorbed at the O/W interface (Fig. 3), which revel their ability to unfold and undertake a conformational change as surface active materials [14,15].

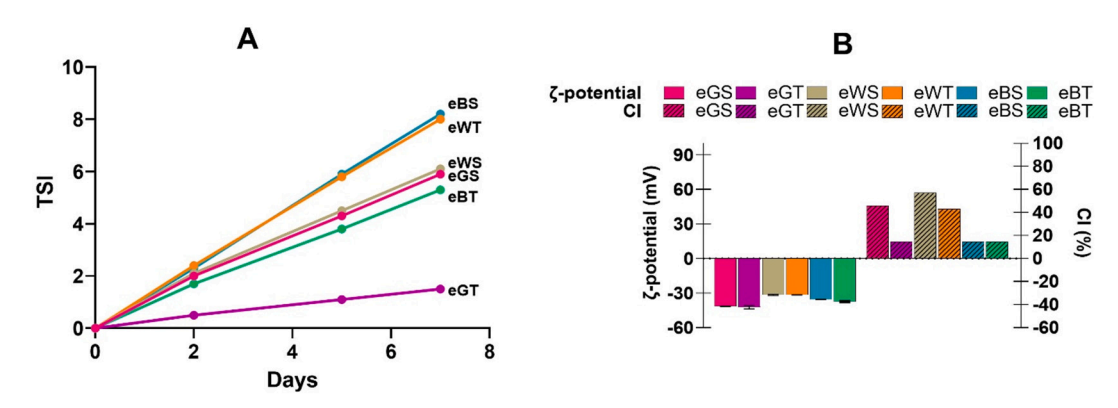


Fig. 7. Emulsions physical stability. A) TSI during storage. B) ζ -potential at day 1 of storage and creaming index (CI) after seven days of storage. Emulsion's code (e) first letter refers to the original side-stream material (defatted grape seed flour (G)), barley spent grains from whisky production (W) and barley spent grains from beer production (B), followed by enzymatic treatment (hydrolysis with subtilisin (S) or trypsin (T)).

 Table 2

 Droplet size of emulsions stabilized with hydrolysates.

	D _[3,2] (μm)		D _[4,3] (μm)		D ₉₀ (μm)		
	Day 0	Day 7	Day 0	Day 7	Day 0	Day 7	
eGS	0.9 ± 0.0^{B}	$1.8 \pm 0.0^{\mathrm{B},\star,+}$	$1.3\pm0.0^{\rm B}$	$2.5\pm0.0^{B,\star}$	$2.6\pm0.0^{\rm B}$	$4.5 \pm 0.0^{C,*}$	
eGT	$2.0 \pm 0.1^{a,b,+}$	$1.7 \pm 0.0^{a,b,_{*}}$	$3.2 \pm 0.0^{\mathrm{b},+}$	$3.2\pm0.1^{\mathrm{b},\star,+}$	$5.3 \pm 0.0^{\mathrm{b,+}}$	$5.7 \pm 0.1^{\mathrm{b},_{\star},+}$	
eWS	$6.7 \pm 0.7^{\mathrm{A},\star,+}$	$3.7 \pm 0.2^{A,B,+}$	$14.2 \pm 0.7^{\text{A}, \star, +}$	$9.0\pm0.9^{\rm A}$	$25.8 \pm 1.0^{\text{A}, \star, +}$	$16.5 \pm 0.4^{A,+}$	
eWT	$5.1\pm0.0^{\mathrm{a},\star}$	$3.2\pm0.2^{\rm a}$	$6.3\pm0.1^{\rm a}$	$13.4 \pm 1.9^{a,\star,+}$	10.7 ± 0.1^a	10.6 ± 0.9^a	
eBS	$0.5 \pm 0.0^{B,+}$	$4.1 \pm 0.4^{\mathrm{A}, \star, +}$	$0.9 \pm 0.1^{B,+}$	$8.3\pm0.5^{\mathrm{A},\star,+}$	$1.8\pm0.1^{\mathrm{B},+}$	$14.9 \pm 0.7^{B,*,+}$	
eBT	$0.4\pm0.0^{\rm b}$	$0.9\pm0.0^{\mathrm{b},\star}$	$0.7\pm0.0^{\rm c}$	$5.0\pm1.2^{\mathrm{b},\star}$	$1.2\pm0.0^{\rm c}$	$6.1\pm0.6^{\mathrm{b},*}$	

Abbreviations: Emulsion's name code means that the first two letters refer to the hydrolysate used to stabilize the emulsion (defatted grape seed flour (eG), barley spent grains from whisky production (eW) and barley spent grains from beer production (eB)), followed by enzymatic treatment applied to the original side-stream material (hydrolysis with subtilisin (S) or trypsin (T)). All results were expressed as means \pm standard deviation (n=6). Different capital letters, at the same column, indicate differences among hydrolysates produced by subtilisin treatment, at the same time of storage. Different small letters, at the same column, indicate differences among hydrolysates produced by trypsin treatment, at the same time of storage. (*) indicate difference between the same emulsion at day 0 and 7 of storage; (+) indicate the difference regarding enzymatic treatment, for a same hydrolysate at the same time of storage. The significance level was p < 0.05 for Kruskal-Wallis, t-test and Wilcoxon test.

3.4. Oxidative stability of emulsions

The oxidative stability of the emulsions was evaluated by determining the formation of primary and secondary oxidation products during storage (Figs. 8 and 9). The extent of oxidation of omega-3 PUFA can increase the content of primary oxidation products or lead to hydroperoxides decomposition, resulting in an increase of secondary oxidation products [13]. In the present study, all emulsions maintained a peroxide concentration below 4 mea O2/kg oil. However, the higher PV in eGT and eBT at day 0 (around 3 m_{eq} O_2/kg oil) may be related to oxidation during emulsion processing (homogenization), which incorporates air and generates heat [48]. Our results show that eBS and eBT were the most oxidized emulsions, with p-anisidine value superior to 20. In contrast, a previous study showed that emulsions stabilized with sunflower and olive meal hydrolysates were more oxidative stable. These authors reported that during 7 days of storage, the PV of the emulsions was higher (around 10 meq O2/kg oil) but peroxides were decomposed into volatiles compounds at a lower rate, resulting in lower p-anisidine value (<6) [48].

Emulsions stabilized with GS presented higher content of hydroperoxides compared with the emulsion stabilized with GT, whereas the opposite was observed for the emulsions stabilized with hydrolysates produced from brewer's spent grains (BS and BT). This finding correlates

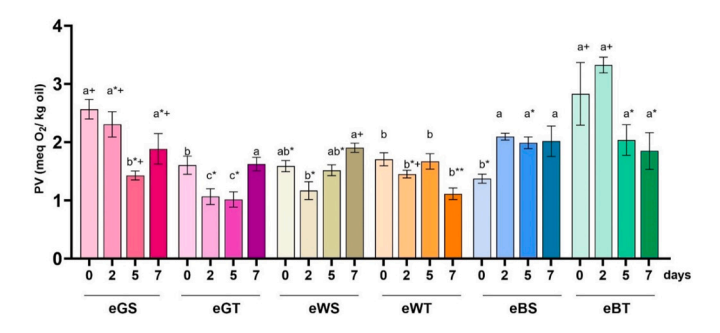


Fig. 8. Primary oxidation products formed in the emulsions during storage (days).

All results were expressed as means \pm standard deviation (n=3). Different small letters represent effect of hydrolysates used to stabilize the emulsion, produced by the same enzymatic treatment at the same time of storage; (*) represents, for the same emulsion, difference among days of storage, (+) represents difference between enzymatic treatment for the same hydrolysates used and time of storage. The significance level was p < 0.05. Emulsion's name code means that the first two letters refer to the hydrolysate used to stabilize the emulsion (defatted grape seed flour (eG), barley spent grains from whisky production (eW) and barley spent grains from beer production (eB)), followed by enzymatic treatment applied to the original side-stream material (hydrolysis with subtilisin (S) or trypsin (T)).

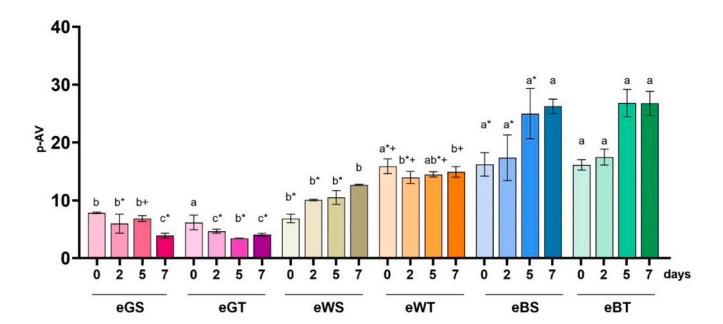


Fig. 9. Secondary oxidation products formed in the emulsions during the storage (days).

All results were expressed as means \pm standard deviation (n = 3). Different small letters represent effect of hydrolysates used to stabilize the emulsion, produced by the same enzymatic treatment at the same time of storage; (+) represents difference between enzymatic treatment for the same hydrolysates used and time of storage; (*) represents, for the same emulsion, difference among days of storage. The significance level was p < 0.05. Emulsion's name code means that the first two letters refer to the hydrolysate used to stabilize the emulsion (defatted grape seed flour (eG), barley spent grains from whisky production (eW) and barley spent grains from beer production (eB)), followed by enzymatic treatment applied to the original side-stream material (hydrolysis with subtilisin (S) or trypsin (T)).

with the smaller droplet size of eGS and eBT emulsions when compared to eGT and eBS, respectively, which implies significant differences in the available specific surface area (Table 2). Indeed, eBS and eBT, due to their smaller droplet size and larger specific area, presented higher p-AV values (Fig. 9). Since all emulsions were prepared at pH > pI, the ferrous ions were attracted to the O/W interface [13]. This, combined with the poor antioxidant capacity of BS and BT hydrolysates (Fig. 2), contributed to higher lipid oxidation as shown in Fig. 9. In contrast, eGS and eGT emulsions, with their larger droplet size, had a smaller specific area, and thus reduced contact area between pro-oxidants and oil where oxidation could be initiated [79]. Moreover, this hydrolysate has presented a remarkable capacity to scavenge radicals and iron chelating (Fig. 2), which has increased emulsion oxidative stability [18].

4. Conclusions

This work shows the feasibility of producing protein-based emulsifiers from side streams of the wine, whisky, and brewing industries. Hydrolysis with trypsin of the studied side streams releases high molecular weight peptides, leading to emulsions with smaller droplet sizes, less flocculation/coalescence, and lower creaming index when compared to hydrolysates produced with subtilisin. Particularly, the

tryptic hydrolysate produced from brewer's spent grains (BT) presented the highest interfacial adsorption and complex dilatational modulus which correlated with a high content of i) high molecular weight peptides and ii) hydrophobic amino acids. Indeed, the emulsion stabilized with BT showed the smallest droplet size and the highest physical stability during storage. However, the high specific area of eBT and lower antioxidant capacity of BT hydrolysate resulted in a lower oxidative stability. Despite the low interfacial adsorption capacity of GT hydrolysate, it resulted in a physically stable emulsion with large droplet size. Thus, the small specific surface area available in this emulsion together with the high antioxidant capacity of GT reduced lipid oxidation in this system. These findings have practical implications for the development of physicochemically stable omega-3 delivery systems by using protein-derived emulsifiers obtained from side streams of the winery and brewery industries.

CRediT authorship contribution statement

Mariana Sisconeto Bisinotto: Writing – original draft, Methodology, Investigation, Formal analysis, Conceptualization. Inar Castro: Writing – review & editing, Supervision, Funding acquisition, Conceptualization. Julia Maldonado-Valderrama: Writing – review & editing, Methodology, Investigation, Formal analysis. Nykola C. Jones: Writing – review & editing, Methodology, Investigation, Formal analysis. Teresa del Castillo-Santaella: Writing – review & editing, Methodology, Investigation. Søren Vrønning Hoffmann: Writing – review & editing, Methodology, Investigation. Emilia M. Guadix: Writing – review & editing, Methodology, Funding acquisition. Pedro J. García-Moreno: Writing – review & editing, Supervision, Methodology, Investigation, Funding acquisition, Conceptualization.

Funding sources

This work was produced with the support of a 2023 Leonardo Grant for Researchers and Cultural Creators, BBVA Foundation. The Foundation takes no responsibility for the opinions, statements, or contents of this project, which are entirely the responsibility of its authors. This work was also funded by the European Union's Horizon 2020 research and innovation programme under grant agreement No 101004806 (MOSBRI-2024-234), and the Coordination for the Improvement of Higher Education Personnel - Brazil (CAPES, Process 88887,831675/ 2023-0). Inar Alves Castro acknowledges funding of the State of São Paulo Research Foundation (FAPESP/Process 2023/14268-7). Julia Maldonado-Valderrama and Teresa del Castillo-Santaella acknowledge support from Ministerio de Ciencia, Innovación y Universidades (PID2023-149387OB-I00) and Consejería de Universidad, Investigación e Innovación and ERDF Andalusia Program 2021-2027 (Grant C-EXP-187-UGR23). Pedro J. García-Moreno and Emilia M. Guadix acknowledge funding from Ministerio de Ciencia, Innovación y Universidades (PID2023-146901OB-I00).

Declaration of competing interest

The authors declare that they have no known competing financial interests or personal relationships that could have appeared to influence the work reported in this paper.

Acknowledgements

We acknowledge the support of the EU H2020 MOSBRI research and innovation programme and the Coordination for the Improvement of Higher Education Personnel – Brazil (CAPES). We are also grateful to Cristina Coronas Lozano for her help in the lab with the production and characterization of emulsions, and to Juan Antonio Holgado Terriza, for supporting us with DINATEN software programming.

Appendix A. Supplementary data

Supplementary data to this article can be found online at https://doi.org/10.1016/j.jibiomac.2025.142736.

Data availability

Data will be made available on request.

References

- [1] G.A. Roth, G.A. Mensah, C.O. Johnson, G. Addolorato, E. Ammirati, L.M. Baddour, N.C. Barengo, A. Beaton, E.J. Benjamin, C.P. Benziger, A. Bonny, M. Brauer, M. Brodmann, T.J. Cahill, J.R. Carapetis, A.L. Catapano, S. Chugh, L.T. Cooper, J. Coresh, V. Fuster, Global burden of cardiovascular diseases and risk factors, 1990–2019: update from the GBD 2019 study, J. Am. Coll. Cardiol. 76 (2020) 2982–3021, https://doi.org/10.1016/j.jacc.2020.11.010.
- [2] World Health Organization, Cardiovascular diseases. https://www.who.int/health-topics/cardiovascular-diseases#tab=tab_1, 2024 (accessed 29 August 2024).
- [3] L. Peter, Inflammation and cardiovascular disease mechanisms, Am. J. Clin. Nutr. 83 (2006) 456S–460S, https://doi.org/10.1093/ajcn/83.2.456S.
- [4] F. Mach, C. Baigent, A.L. Catapano, K.C. Koskina, M. Casula, L. Badimon, M. J. Chapman, G.G. de Backer, V. Delgado, B.A. Ference, I.M. Graham, A. Halliday, U. Landmesser, B. Mihaylova, T.R. Pedersen, G. Riccardi, D.J. Richter, M. S. Sabatine, M.R. Taskinen, R.S. Patel, ESC/EAS guidelines for the management of dyslipidaemias: lipid modification to reduce cardiovascular risk, Atherosclerosis 290 (2019) (2019) 140–205, https://doi.org/10.1016/j. atherosclerosis.2019.08.014.
- [5] D.R. Tocher, M.B. Betancor, M. Sprague, R.E. Olsen, J.A. Napier, Omega-3 long-chain polyunsaturated fatty acids, EPA and DHA: bridging the gap between supply and demand, Nutrients 11 (2019) 1–20, https://doi.org/10.3390/nu11010089.
- [6] J.K. Innes, P.C. Calder, Marine omega-3 (N-3) fatty acids for cardiovascular health: an update for 2020, Int. J. Mol. Sci. 21 (2020) 1–21, https://doi.org/10.3390/ ijms21041362.
- [7] S. Ghelichi, M. Hajfathalian, P.J. García-Moreno, B. Yesiltas, A.D. Moltke-Sørensen, C. Jacobsen, Food enrichment with omega-3 polyunsaturated fatty acids, in: P. J. García-Moreno, C. Jacobsen, A.D.M. Sørensen, B. Yesiltas (Eds.), Omega-3 Delivery Systems: Production, Physical Characterization and Oxidative Stability, Academic Press, London, 2021, pp. 395–425.
- [8] P. Prasad, P. Anjali, R.V. Sreedhar, Plant-based stearidonic acid as sustainable source of omega-3 fatty acid with functional outcomes on human health, Crit. Rev. Food Sci. Nutr. 61 (2021) 1725–1737, https://doi.org/10.1080/ 1040820823020317455137
- [9] E.J. Baker, E.A. Miles, G.C. Burdge, P. Yaqoob, P.C. Calder, Metabolism and functional effects of plant-derived omega-3 fatty acids in humans, Prog. Lipid Res. 64 (2016) 30–56, https://doi.org/10.1016/j.plipres.2016.07.002.
- [10] M.S. Nogueira, B. Scolaro, G.L. Milne, I.A. Castro, Oxidation products from omega-3 and omega-6 fatty acids during a simulated shelf life of edible oils, LWT 101 (2019) 113–122, https://doi.org/10.1016/j.lwt.2018.11.044.
- [11] C. Jacobsen, P.J. García-Moreno, B. Yesiltas, A.D. Moltke-Sørensen, Lipid oxidation and traditional methods for evaluation, in: P.J. García-Moreno, C. Jacobsen, A.D. M. Sørensen, B. Yesiltas (Eds.), Omega-3 Delivery Systems: Production, Physical Characterization and Oxidative Stability, Academic Press, London, 2021, pp. 183–200.
- [12] A.D. Moltke-Sørensen, P.J. García-Moreno, B. Yesiltas, C. Jacobsen, Introduction to delivery systems and stability issues, in: P.J. García-Moreno, C. Jacobsen, A.D. M. Sørensen, B. Yesiltas (Eds.), Omega-3 Delivery Systems: Production, Physical Characterization and Oxidative Stability, Academic Press, London, 2021, pp. 107-117
- [13] M. Hennebelle, P. Villeneuve, E. Durand, J. Lecomte, J. van Duynhoven, A. Meynier, B. Yesiltas, C. Jacobsen, C. Berton-Carabin, Lipid oxidation in emulsions: new insights from the past two decades, Prog. Lipid Res. 94 (2024) e101275, https://doi.org/10.1016/j.plipres.2024.101275.
- [14] P.J. García-Moreno, J. Yang, S. Gregersen, N.C. Jones, C.C. Berton-Carabin, L.M. C. Sagis, S.V. Hoffmann, P. Marcatili, M.T. Overgaard, E.B. Hansen, C. Jacobsen, The structure, viscoelasticity and charge of potato peptides adsorbed at the oilwater interface determine the physicochemical stability of fish oil-in-water emulsions, Food Hydrocoll. 115 (2021) e106605, https://doi.org/10.1016/j.foodhyd.2021.106605.
- [15] R. Pérez-Gálvez, J. Maldonado-Valderrama, N.C. Jones, S.V. Hoffmann, E. Guadix, P.J. García-Moreno, Influence of the enzymatic treatment and pH on the interfacial and emulsifying properties of sunflower and olive protein hydrolysates, Food Hydrocoll. 154 (2024) e110135, https://doi.org/10.1016/j.foodhyd.2024.110135.
- [16] S. Drusch, M. Klost, H. Kieserling, Current knowledge on the interfacial behaviour limits our understanding of plant protein functionality in emulsions, Curr. Opin. Colloid Interface Sci. 56 (2021) e101503, https://doi.org/10.1016/j. cocis.2021.101503.
- [17] C. Liu, M. Bhattarai, K.S. Mikkonen, M. Heinonen, Effects of enzymatic hydrolysis of fava bean protein isolate by Alcalase on the physical and oxidative stability of oil-in-water emulsions, J. Agri. Food Chem. 67 (2019) 6625–6632, https://doi.org/ 10.1021/acs.jafc.9b00914.
- [18] M. Hadidi, F. Aghababaei, D.J. Gonzalez-Serrano, G. Goksen, M. Trif, D. J. McClements, A. Moreno, Plant-based proteins from agro-industrial waste and by-

- products: towards a more circular economy, Int. J. Biol. Macromol. 261 (2024) e129576, https://doi.org/10.1016/j.ijbiomac.2024.129576.
- [19] Statista, Alcoholic drinks worldwide. https://www.statista.com/outlook/cmo/alcoholic-drinks/worldwide, 2024 (accessed 6 September 2024).
- [20] E.C. Umego, C. Barry-Ryan, Review of the valorization initiatives of brewing and distilling by-products, Crit. Rev. Food Sci. Nutr. 64 (2023) 8231–8247, https://doi. org/10.1080/10408398.2023.2198012.
- [21] C. Alvarez-Ossorio, M. Orive, E. Sanmartín, S. Alvarez-Sabatel, J. Labidi, J. Zufia, C. Bald, Composition and techno-functional properties of grape seed flour protein extracts, ACS Food Sci Technol. 2 (2022) 125–135, https://doi.org/10.1021/ acsfoodscitech.1c00367.
- [22] B. Antonić, S. Jančíková, D. Dordević, B. Tremlová, Grape pomace valorization: a systematic review and meta-analysis, Foods 9 (2020) e1627, https://doi.org/ 10.3390/foods9111627.
- [23] Y.L. Chin, J.K. Keppler, S.T. Dinani, W.N. Chen, R. Boom, Brewers' spent grain proteins: the extraction method determines the functional properties, Innov. Food Sci. Emerg. Technol. 94 (2024) e103666, https://doi.org/10.1016/j. ifset.2024.103666.
- [24] L. Nyhan, A.W. Sahin, H.H. Schmitz, J.B. Siegel, E.K. Arendt, Brewers' spent grain: an unprecedented opportunity to develop sustainable plant-based nutrition ingredients addressing global malnutrition challenges, J Agri Food Chem. 71 (2023) 10543–10564, https://doi.org/10.1021/acs.jafc.3c02489.
- [25] S.R. Garcia, J.C. Orellana-Palacios, D.J. McClements, A. Moreno, M. Hadidi, Sustainable proteins from wine industrial by-product: ultrasound-assisted extraction, fractionation, and characterization, Food Chem. 455 (2024) e139743, https://doi.org/10.1016/j.foodchem.2024.139743.
- [26] I. Celus, K. Brijs, J.A. Delcour, Enzymatic hydrolysis of brewers' spent grain proteins and technofunctional properties of the resulting hydrolysates, J. Agric. Food Chem. 55 (2007) 8703–8710, https://doi.org/10.1021/jf071793c.
- [27] Y.L. Chin, K.F. Chai, W.N. Chen, Upcycling of brewers' spent grains via solid-state fermentation for the production of protein hydrolysates with antioxidant and techno-functional properties, Food Chem X 13 (2022) e100184, https://doi.org/ 10.1016/j.fochx.2021.100184.
- [28] M. Kriisa, A. Taivosalo, M. Föste, M.L. Kütt, M. Viirma, R. Priidik, M. Korzeniowska, Y. Tian, O. Laaksonen, B. Yang, R. Vilu, Effect of enzyme-assisted hydrolysis on brewer's spent grain protein solubilization – peptide composition and sensory properties, Appl Food Res. 2 (2022) e100108, https://doi.org/ 10.1016/j.afres.2022.100108.
- [29] G.C.G. Carlini, G.G. Roschel, R.A. Ferrari, S.M. Alencar, H.C. Ota, T.F.F. da Silveira, I.A. Castro, Chemical characterization of Echium plantagineum seed oil obtained by three methods of extraction, J Food Sci 12 (2021) 5307–5317, https://doi.org/ 10.1111/1750-3841.15972.
- [30] M.S. Bisinotto, L.D. Chedid, A.D.S. Gouveia, H.J.O. Ramos, I.A. Castro, Oxidative stability of Echium crude oil during cold-press extraction process, Italian J of Food Sci 37 (2025), https://doi.org/10.15586/ijfs.v37i2.2878.
- [31] Z. Qazanfarzadeh, A.R. Ganesan, L. Mariniello, L. Conterno, V. Kumaravel, Valorization of brewer's spent grain for sustainable food packaging, J. Clean. Prod. 385 (2023) e135726, https://doi.org/10.1016/j.jclepro.2022.135726.
- [32] M.J. Cejudo-Bastante, M. Oliva-Sobrado, M.L. González-Miret, F.J. Heredia, Optimisation of the methodology for obtaining enzymatic protein hydrolysates from an industrial grape seed meal residue, Food Chem. 370 (2022) e131078, https://doi.org/10.1016/j.foodchem.2021.131078.
- [33] P.J. García-Moreno, A. Guadix, E.M. Guadix, C. Jacobsen, Physical and oxidative stability of fish oil-in-water emulsions stabilized with fish protein hydrolysates, Food Chem. 203 (2016) 124–135, https://doi.org/10.1016/j. foodchem.2016.02.073.
- [34] A. Ballon, L.S. Queiroz, S. de Lamo-Castellví, C. Güell, M. Ferrando, C. Jacobsen, B. Yesiltas, Physical and oxidative stability of 5% fish oil-in-water emulsions stabilized with lesser mealworm (Alphitobius diaperinus larva) protein hydrolysates pretreated with ultrasound and pulsed electric fields, Food Chem. 476 (2025) 143339, https://doi.org/10.1016/J.FOODCHEM.2025.143339.
- [35] R. Morales-Medina, F. Tamm, A.M. Guadix, E.M. Guadix, S. Drusch, Functional and antioxidant properties of hydrolysates of sardine (S. pilchardus) and horse mackerel (T. mediterraneus) for the microencapsulation of fish oil by spray-drying, Food Chem. 194 (2016) 1208–1216, https://doi.org/10.1016/J. FOODCHEM 2015 08 122
- [36] F. Tamm, K. Gies, S. Diekmann, Y. Serfert, T. Strunskus, A. Brodkorb, S. Drusch, Whey protein hydrolysates reduce autoxidation in microencapsulated long chain polyunsaturated fatty acids, Eur. J. of Lipid Sci and Technol 12 (1960–1970), https://doi.org/10.1002/eilt.201400574.
- [37] F. Camacho, P. González-Tello, M.P. Páez-Dueñas, E.M. Guadix, A. Guadix, Correlation of base consumption with the degree of hydrolysis in enzymic protein hydrolysis, J. Dairy Res. 68 (2001) 251–265, https://doi.org/10.1017/ s0022029901004824.
- [38] W. Horwitz, G.W. Latimer Jr., Official Methods of Analysis, seventeenth ed., AOAC International, Maryland, 2008.
- [39] J. Lazarević, I. Čabarkapa, S. Rakita, M. Banjac, Z. Tomičić, D. Škrobot, G. Radivojević, B.K. Pivarski, D. Tešanović, Invasive crayfish faxonius limosus: meat safety, nutritional quality and sensory profile, Int. J. Environ. Res. Public Health 19 (2022) e16819, https://doi.org/10.3390/ijerph192416819.
- [40] M.S. Bisinotto, D.C. da Silva, L.C. Fino, F.M. Simabuco, R.M.N. Bezerra, A.E. C. Antunes, M.T.B. Pacheco, Bioaccessibility of cashew nut kernel flour compounds released after simulated *in vitro* human gastrointestinal digestion, Food Res. Int. 139 (2021) 109906, https://doi.org/10.1016/j.foodres.2020.109906.
- [41] P.J. García-Moreno, I. Batista, C. Pires, N.M. Bandarra, F.J. Espejo-Carpio, A. Guadix, E.M. Guadix, Antioxidant activity of protein hydrolysates obtained from

- discarded Mediterranean fish species, Food Res. Int. 65 (2014) 469–476, https://doi.org/10.1016/j.foodres.2014.03.061.
- [42] N.E. Rahmani-Manglano, N.C. Jones, S.V. Hoffmann, E.M. Guadix, R. Pérez-Gálvez, A. Guadix, P.J. García-Moreno, Structure of whey protein hydrolysate used as emulsifier in wet and dried oil delivery systems: effect of pH and drying processing, Food Chem. 390 (2022) e133169, https://doi.org/10.1016/j. foodchem. 2022. 133169.
- [43] A.J. Miles, F. Wien, B.A. Wallace, Redetermination of the extinction coefficient of camphor-10-sulfonic acid, a calibration standard for circular dichroism spectroscopy, Anal. Biochem. 335 (2004) 338–339, https://doi.org/10.1016/j. ab 2004 08 035
- [44] J.M. Ruiz-Álvarez, T. Castillo-Santaella, J. Maldonado-Valderrama, A. Guadix, E. M. Guadix, P.J., García-Moreno, pH influences the interfacial properties of blue whiting (M. poutassou) and whey protein hydrolysates determining the physical stability of fish oil-in-water emulsions, Food Hydrocoll. 122 (2022) e107075, https://doi.org/10.1016/j.foodhyd.2021.107075.
- [45] J. Maldonado-Valderrama, A. Torcello-Gómez, T. Castillo-Santaella, J.A. Holgado-Terriza, M.A. Cabrerizo-Vilchez, Subphase exchange experiments with the pendant drop technique, Adv. Colloid Interface Sci. 222 (2015) 488–501, https://doi.org/10.1016/j.cis.2014.08.002.
- [46] J. Maldonado-Valderrama, A. Martín-Rodriguez, M.J. Gálvez-Ruiz, R. Miller, D. Langevin, M.A. Cabrerizo-Vílchez, Foams and emulsions of β-casein examined by interfacial rheology, Colloids Surf. A Physicochem. Eng. Asp. 323 (2008) 116–122, https://doi.org/10.1016/j.colsurfa.2007.11.003.
- [47] M. Padial-Domínguez, F.J. Espejo-Carpio, P.J. García-Moreno, C. Jacobsen, E. M. Guadix, Protein derived emulsifiers with antioxidant activity for stabilization of omega-3 emulsions, Food Chem. 329 (2020) e110135, https://doi.org/10.1016/j.foodchem.2020.127148.
- [48] J.L. Ospina-Quiroga, C. Coronas-Lozano, P.J. García-Moreno, E.M. Guadix, M. C. Almécija-Rodríguez, R. Pérez-Gálvez, Use of olive and sunflower protein hydrolysates for the physical and oxidative stabilization of fish oil-in-water emulsions, J. Sci. Food Agric. 104 (2024) 5541–5552, https://doi.org/10.1002/isfa.13384.
- [49] O. Mengual, G. Meunier, I. Cayré, K. Puech, P. Snabre, TURBISCAN MA 2000: multiple light scattering measurement for concentrated emulsion and suspension instability analysis, Talanta 50 (1999) 445–456.
- [50] K. Wang, G. Li, B. Zhang, Opposite results of emulsion stability evaluated by the TSI and the phase separation proportion, Colloids Surf. A Physicochem. Eng. Asp. 558 (2018) 402–409, https://doi.org/10.1016/j.colsurfa.2018.08.084.
- [51] N.C. Shantha, E.A. Decker, Rapid, sensitive, iron-based spectrophotometric methods for determination of peroxide values of food lipids, J of AOAC Int. 77 (1994) 421–424, https://doi.org/10.1093/jaoac/77.2.421.
- [52] ISO, ISO 6885:2006(en): animal and vegetable fats and oils determination of anisidine value. https://www.iso.org/obp/ui/#iso:std:iso:6885:ed-4:v1:en, 2006 (accessed 15 February 2024).
- [53] E. Durand, S. Beaubier, I. Ilic, F. Fine, R. Kapel, P. Villeneuve, Production and antioxidant capacity of bioactive peptides from plant biomass to counteract lipid oxidation, Curr. Res. Food Sci. 4 (2021) 365–397, https://doi.org/10.1016/j. crfs.2021.05.006.
- [54] J.L. Ospina-Quiroga, P.J. García-Moreno, A. Guadix, E.M. Guadix, M.D. C. Almécija-Rodríguez, R. Pérez-Gálvez, Evaluation of plant protein hydrolysates as natural antioxidants in fish oil-in-water emulsions, Antioxidants 11 (2022) 1–18, https://doi.org/10.3390/antiox11081612.
- [55] J.V. Olsen, S.E. Ong, M. Mann, Trypsin cleaves exclusively C-terminal to arginine and lysine residues, Mol. Cell. Proteomics 3 (2004) 608–614, https://doi.org/ 10.1074/mcp.T400003-MCP200.
- [56] M. Houde, N. Khodaei, N. Benkerroum, S. Karboune, Barley protein concentrates: extraction, structural and functional properties, Food Chem. 254 (2018) 367–376, https://doi.org/10.1016/j.foodchem.2018.01.156.
- [57] I. Celus, K. Brijs, J.A. Delcour, The effects of malting and mashing on barley protein extractability, J. Cereal Sci. 44 (2006) 203–211, https://doi.org/10.1016/j. jcs.2006.06.003.
- [58] D. Gazzola, S. Vincenzi, L. Gastaldon, S. Tolin, G. Pasini, A. Curioni, The proteins of the grape (Vitis vinifera L.) seed endosperm: fractionation and identification of the major components, Food Chem. 155 (2014) 132–139, https://doi.org/10.1016/j. foodchem.2014.01.032.
- [59] P.J. García-Moreno, B. Yesiltas, S.G. Echers, P. Marcatili, M.T. Overgaard, E. B. Hansen, C. Jacobsen, Recent advances in the production of emulsifying peptides with the aid of proteomics and bioinformatics, Curr. Opin. Food Sci. 51 (2023) e101039, https://doi.org/10.1016/j.cofs.2023.101039.
- [60] P.J. García-Moreno, S. Gregersen, E.R. Nedamani, et al., Identification of emulsifier potato peptides by bioinformatics: application to omega-3 delivery emulsions and release from potato industry side streams, Sci. Rep. 10 (2020) 690, https://doi.org/ 10.1038/s41598.019.57229.6
- [61] Y. Wang, Z. Li, H. Li, C. Selomulya, Effect of hydrolysis on the emulsification and antioxidant properties of plant-sourced proteins, Curr. Opin. Food Sci. 48 (2022) e100949, https://doi.org/10.1016/j.cofs.2022.100949.
- [62] A.M. Ghribi, I. Maklouf Gafsi, A. Sila, C. Blecker, S. Danthine, H. Attia, A. Bougatef, S. Besbes, Effects of enzymatic hydrolysis on conformational and functional properties of chickpea protein isolate, Food Chem. 187 (2015) 322–330, https:// doi.org/10.1016/j.foodchem.2015.01.156.
- [63] A.G.P. Samaranayaka, E.C.Y. Li-Chan, Food-derived peptidic antioxidants: a review of their production, assessment, and potential applications, J. Funct. Foods 3 (2011) 229–254, https://doi.org/10.1016/j.jff.2011.05.006.

- [64] S. Olivares-Galván, M.L. Marina, M.C. García, Extraction of valuable compounds from brewing residues: malt rootlets, spent hops, and spent yeast, Trends Food Sci. Technol. 127 (2022) 181–197, https://doi.org/10.1016/j.tifs.2022.06.002.
- [65] M. Iuga, S. Mironeasa, Potential of grape byproducts as functional ingredients in baked goods and pasta, Compr. Rev. Food Sci. Food Saf. 19 (2020) 2473–2505, https://doi.org/10.1111/1541-4337.12597.
- [66] A.J. Miles, B.A. Wallace, Circular dichroism spectroscopy of membrane proteins, Chem. Soc. Rev. 45 (2016) 4859–4872, https://doi.org/10.1039/c5cs00084j.
- [67] A. Schröder, C. Berton-Carabin, P. Venema, L. Cornacchia, Interfacial properties of whey protein and whey protein hydrolysates and their influence on O/W emulsion stability, Food Hydrocoll. 73 (2017) 129–140, https://doi.org/10.1016/j. foodhyd.2017.06.001.
- [68] X. Zhang, Q. Wang, Z. Liu, L. Zhi, B. Jiao, H. Hu, X. Ma, D. Agyei, A. Shi, Plant protein-based emulsifiers: mechanisms, techniques for emulsification enhancement and applications, Food Hydrocoll. 144 (2023) e109008, https://doi.org/10.1016/j. foodbyd.2023.109008.
- [69] M.M.G. de Oliveira, A.G.B.W. Fessori, V.J. Huamaní-Meléndez, S.L. Ferreira Júnior, Í.P. Caruso, M.A. Mauro, Prospects of cowpea protein as an alternative and natural emulsifier for food applications: effect of pH and oil concentration, Int. J. Biol. Macromol. 296 (2025) e139727, https://doi.org/10.1016/j. iibiomac.2025.139727
- [70] A.M.M. da Silva, F.S. Almeida, M.F. da Silva, R. Goldbeck, A.C.K. Sato, How do pH and temperature influence extraction yield, physicochemical, functional, and rheological characteristics of brewer spent grain protein concentrates? Food Bioprod. Process. 139 (2023) 34–45, https://doi.org/10.1016/j.fbp.2023.03.001.
- [71] X. Zhang, J. Hao, D. Ma, Z. Li, S. Zhang, Y. Li, Alcalase-hydrolyzed insoluble soybean meal hydrolysate aggregates: structure, bioactivity, function properties, and influences on the stability of oil-in-water emulsions, Int. J. Biol. Macromol. 265 (2024) e131014, https://doi.org/10.1016/j.ijbiomac.2024.131014.

- [72] L.M.C. Sagis, K.N.P. Humblet-Hua, S.E.H.J. Van Kempen, Nonlinear stress deformation behavior of interfaces stabilized by food-based ingredients, J. Condens. Matter Phys. 26 (2014) e464105, https://doi.org/10.1088/0953-8984/26/46/464105.
- [73] J. Yang, I. Thielen, C.C. Berton-Carabin, E. van der Linden, L.M.C. Sagis, Nonlinear interfacial rheology and atomic force microscopy of air-water interfaces stabilized by whey protein beads and their constituents, Food Hydrocoll. 101 (2020) e105466, https://doi.org/10.1016/j.foodhyd.2019.105466.
- [74] L.M. Sagis, J. Yang, Protein-stabilized interfaces in multiphase food: comparing structure-function relations of plant-based and animal-based proteins, Curr. Opin. Food Sci. 43 (2022) 53–60, https://doi.org/10.1016/j.cofs.2021.11.003.
- [75] D.J. McClements, J. Lu, L. Grossmann, Proposed methods for testing and comparing the emulsifying properties of proteins from animal, plant, and alternative sources, Colloids Interfaces 6 (2022) 1–45, https://doi.org/10.3390/ colloids6020019.
- [76] C. Du, Y. Cai, T. Liu, L. Huang, Z. Long, M. Zhao, Y. Zhang, Q. Zhao, Physicochemical, interfacial and emulsifying properties of insoluble soy peptide aggregate: effect of homogenization and alkaline-treatment, Food Hydrocoll. 109 (2020) e106125, https://doi.org/10.1016/j.foodhyd.2020.106125.
- [77] M.C. Figueroa-Espinoza, A. Zafimahova, P.G.M. Alvarado, E. Dubreucq, C. Poncet-Legrand, Grape seed and apple tannins: emulsifying and antioxidant properties, Food Chem. 178 (2015) 38-44, https://doi.org/10.1016/j.foodchem.2015.01.056.
- [78] M. Li, D.J. McClements, X. Liu, F. Liu, Design principles of oil-in-water emulsions with functionalized interfaces: mixed, multilayer, and covalent complex structures, Compr Rev Food Sci Food Saf. 19 (2020) 3159–3190, https://doi.org/10.1111/ 1541.4337 12622
- [79] S. Ghelichi, M. Hajfathalian, B. Yesiltas, A.D.M. Sørensen, P.J. García-Moreno, C. Jacobsen, Oxidation and oxidative stability in emulsions, Compr. Rev. Food Sci. Food Saf. 22 (2023) 1864–1901, https://doi.org/10.1111/1541-4337.13134.